The Institute of Space and Astronautical Science
Report No. 612, June 1984

Experimental Study on Porous-Plug Phase Separator for Superfluid Hell

By

Masahide MURAKAMI*, Noriyuki NAKANIWA**, Hirotaka NAKAI*
and Kiichiro UYAMA***

(April 5, 1984)

Summary: Superfluid liquid helium II (HeII) has been requested for cooling of such space borne instruments as infrared detectors down to absolute zero. A phase separator composes of a crucial part of such cryogenic systems to allow the liquid phase to be separated from the vapor in order to safely contain HeII in containers in the zero-gravity state. In the present investigation, porous-plugs were fabricated and tested to understand the basic flow characteristics through porous-plugs both in the loboratory and in the zero-gravity state aboard a rocket. Results show that the phase separation and the cooling power control were satisfactorily performed in both situations. The fundamental feature of the flow phenomena through porous-plugs is made clear quantitatively as well as qualitatively to provide sufficient data for the practical design of porous-plugs for potential space borne IR telescope systems.

I. INTRODUCTION

A variety of space missions, including infrared astronomical observation missions, have requested cooling technique down to absolute zero. Liquid nelium is a natural choice for such purposes, and superfluid helium (HeII) is especially suitable because of the lowest temperature and of the excellent cooling capability [*1*]. However, HeII may easily escape from a container into venting lines in the low- or zero-gravity situation, as the vapor-liquid phase boundary surface can no be well defined in containers under such conditions. A phase separator is of crucial importance for the efficient containment of HeII for space missions. Two kinds of phase separators have been proposed and investigated. One is designated as a porous-plug which is composed of porous media, and another as an active phase separator (APS). The latter possesses a capability for the active flow rate control by adjusting the overlapping length of a narrow gap between two concentric cylinders, while the former is basically of fixed conductance. Active phase separators have been proposed and tested in conjunction with the German Infrared Laboratory (GIRL) project [*2* and *3*]. It was reported that an APS could work as a key device to control both the flow rate (cooling power) and the temperature. However, it seems rather sensitive to the acceleration and the vibration during the powered flight,

* Inst. of Structural Eng., University of Tsukuba.
** Nissan Motor Co. Ltd.
*** Toshiba Corporation, Fuchu Works.

because it composes of several mechanical parts to drive the inner cylinder. A solenoid driver may generate large amount of heat. Thus, an APS does not necessarily seem to be the unique choice as a phase separator. On the other hand, a porous-plug is much simpler in the structure and thus more reliable. This has long been tested by the JPL group [*4* and *5*] as well as by the NASA Marshall group [*6* and *7*]. Moreover, the feasibility of the control of flow rate through porous-plugs by the use of an electric heater was confirmed experimentally by Murakami *et al.* [*8*].

The present study was initiated in connection with the basic research for the Infrared Telescope in Space (IRTS) project [*9*], when the fundamental flow characteristics through porous-plugs was not so clear and thus the design data were not fully available. The details on the method of flow rate control by the use of a heater were not completely understood. It was found in the preliminary stage of this study [*8*] that the steady flow characteristics did not necessarily agree with the thoretical prediction which may be considered as a porous-plug version of the theory presented by Shotte [*10, 11* and *12*]. Thus, the purposes of this study were defined as follows; i) to reveal the fundamental flow characteristics through porous-plugs, ii) to investigate a method of flow rate control, by the use of a heater, iii) to perform a zero-g test aboard a rocket. The preliminary results were already presented in Ref. [28]. In this report, a full description of the study will be given including the zero-g test data. In the next capter, chapter 2, the experimental porous-plugs and apparatus are described. The general flow characteristics through porous-plugs is explained in the first section of chapter 3, and several particular experiments for further understanding of the details are reported in the following sections. The results of experiments of the flow rate control are given in chapter 4, and the rocket flight experiment is reported in chapter 5. In the last chapter, chapter 6, a number of conclusions are described.

II. Experimental Porous-Plugs and Apparatus

2.1 Porous-Plugs

The key mechanism to separate the vapor phase from the liquid HeII is the thermomechanical effect acting on the super component due to the temperature difference across a porous-plug. That is, the super component is driven toward the upstream side where the temperature is higher than that at the downstream side where HeII is evaporating. Consequently, the net flow rate of HeII may be enough reduced to prevent bulk liquid HeII from leaking out through a plug, because the super component flows in the opposite direction to the net flow. The liquid-vapor phase boundary surface must be formed somewhere inside of a plug as far as it is activated. Porous-plugs are made of such porous materials as ceramic alumina and sintered stainless steel, whose pore sizes are of the order of one micron meter or less. This is not so fine as a super leak, and the normal (viscous) component can flow through it. The flow conductance of a porous-plug is of fixed value, and thus it possesses essentially no active capability for the flow rate control. However, it has been demonstrated that the control was feasible not by any mechanical means but by a thermal one by the use of a heater mounted on the downstream side of a porous-plug [*8*].

Table 1. Basic parameters of experimental porous-plugs

No.	1	2	3	4	5	6	7
Material	Ceramic Alumina				Sintered Stainless Steel		
Area A ($\times 10^{-4}m^2$)	3.80	3.80	3.80	2.10	1.92	1.92	1.92
Thickness t ($\times 10^{-3}m$)	7.0	10.0	15.0	5.0	1.5	1.5	1.5
Permeability K ($\times 10^{-14}m^2$)	12.2	9.45	6.37	5.52	3.52	1.70	1.70
Porosity ϵ	0.375	0.375	0.404	0.375	0.325	0.325	0.325
Pore Radius $\bar{R}$ ($\times 10^{-6}m$)	*	1.5	1.1	*	*	3.8	3.8

* not available.

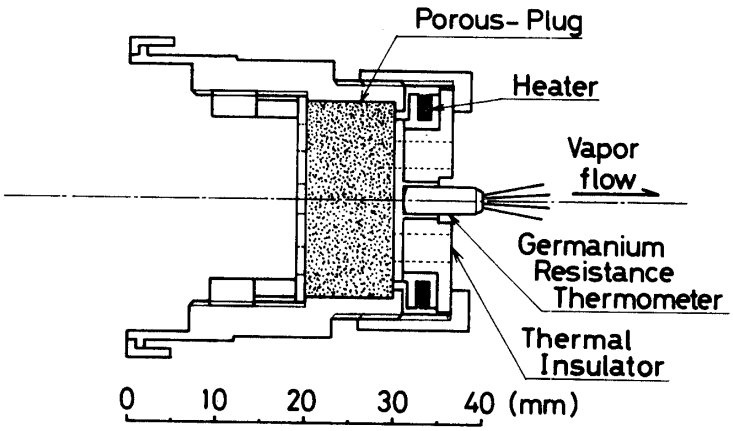

Fig. 1. Structure of porous-plug and porous-plug mount.

The basic parameters of experimental porous-plugs used in the present study are listed in Table-1. Some were made of ceramic alumina, and others of sintered stainless steel, which were a modified version of NUPRO air filter (SS-8F-P4-2). Disk shaped porous-plug elements were fixed to mount with STYCAST 2850 GT for leak-tight as, for example, illustrated in Fig. 1. A germanium resistance thermometer was contacted with the downstream side of plug, and a manganin heater winding (130Ω) was fitted, which was designed to supply heat to the downstream side to test the capability of the flow rate control. A radiation shield was installed above the mount to cut the radiation heat input from the 300K-portions. The mount was soldered to a vapor evacuation pipe at the bottom by Wood's metal.

A mercury porosimeter (CARLO ERBA) was utilized to measure the mean pore radius and the porosity of each porous-plug sample. The detail is described by Nakaniwa [*13*]. This porosimeter applies the pressurized-mercury-method to get the pore distribution. The distribution is given as a unique function of the pressure and the volume into which mercury enters. The porosity is directly derived from the final volume of entered mercury at the maximum pressure (about 200 MPa), by dividing it by the bulk volume of

the smaple which is measured prior to the pressurization. This is also given by the ratio of the sample mass to the product of the material density of the porous substrate and the bulk volume. The agreement between the two was found to be fairly good. The pore diameter of each sample was widely distributed, typically from several microns down to submicrons. Thus, the mean pore size was defined as the expected value of the pore diameter calculated by the numerical integration of the distribution curve.

The permeability was experimentally determined by forced air flow test under the room temperature condition. The test were carried out by the use of the same apparatus as the HeII experiment, except that the upstream side of a plug was exposed to the atmospheric air. The permeability, K, was calculated from the data by applying the formula;

$$K=\frac{\dot{V}\eta}{A(\Delta p/l)}, \tag{1}$$

where the volumetric air flow rate, $\dot{V}$, and the pressure difference across a plug, Δp, were measured. A, l and η are the plug cross sectional area, the thickness and the air viscosity, respectively. The test results, actually, exhibited a linear relation between $\dot{V}$ and Δp for small $\dot{V}$, and thus the gradient ws employed for the calculation. It is well known that these quantities, the permeability, the porosity ϵ, and the mean pore ratius $\bar{R}$ can be correlated in an empirical form, the Blake-Kozeny equation [*14*].

$$K=\frac{(2\bar{R}/0.41)^2\epsilon^3}{150(1-\epsilon)^2}. \tag{2}$$

To derive this equation, it is assumed that the gas flows in the space which is made by packing small spheres of a radius r and that another empirical relation $r=\bar{R}/0.41$ is valid. A comparison between values obtained both from the air flow test and from the Blake-Kozeny equation shows that the agreement is fair as shown in Ref. 13.

The principle of phase separation through a porous-plug is formulated on the basis of the two fluid model of superfluid proposed by Landau [*15*]. The theory of flow through a porous-plug is considered for the model illustrated in Fig. 2. It should be noted that this model corresponds to an ideal case when the vapor-liquid phase boundary just coincides with the surface of the downstream side of a plug. The upstream side of the plug directly contacts with bulk HeII in the bath, and the downstream side is introduced to the vapor evacuation pipe. The two-fluid theory assumes that the superfluid is composed of both the normal component and the super, each of which flows independently. The two-fluid equations are rather simple provided that higher order terms are neglected and HeII is assumed to be incompressible. The equation of motion of the normal component is;

$$\rho_n \frac{D\bar{v}_n}{Dt}=-\frac{\rho_n}{\rho}\nabla p-\rho_s S\nabla T+\eta_n\nabla^2 v_n \tag{3}$$

and of the super component;

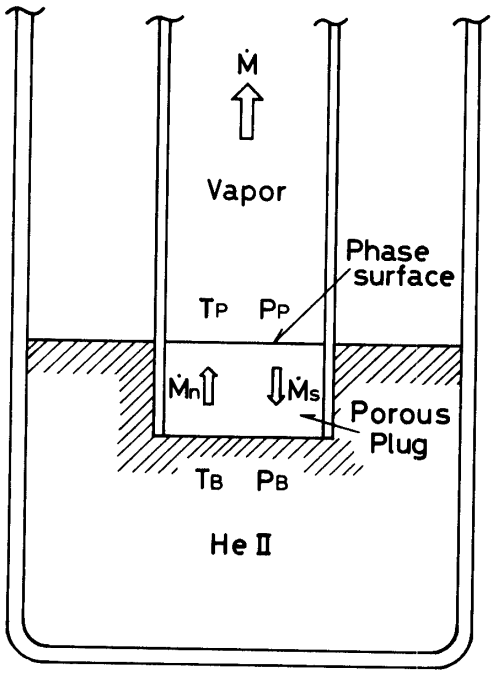

Fig. 2. Theoretical model of phase separation of HeII through porous-plugs.

$$\rho_s \frac{D\bar{v}_s}{Dt} = -\frac{\rho_s}{\rho}\nabla p + \rho_s S \nabla T. \tag{4}$$

Here, ρ, ρ_n and ρ_s are the total density, the normal component density and the super component density, respectively, and $\bar{v}_n$ and $\bar{v}_s$ are the velocities of the normal and the super components, respectively. p is the pressure, T the temerature, S the specific entropy, and η_n the normal component viscosity. D/Dt denotes the substantial derivative. It is assumed that the flow through a plug is one-dimensional and steady and the the mass flow rate, $\dot{M}/A$ is small, where A is the cross sectional area of a plug. Furthermore, it is also postulated that any parasitic heat leak and heat transfer by conduction through plug material are negligibly small. The restriction on the amount of $\dot{M}/A$ assures that the HeII flow through a plug is free from the mutual friction between the super and the normal components. Under these conditions, the equations (3) and (4) reduce to a simple form as

$$\nabla p = \eta_n \nabla^2 v_n. \tag{5}$$

This suggests that the pressure drop results from the normal flow, just as in usual viscous flows. Now it should be noted that the treatment is one-dimensional, though the same notations are used as in the three-dimensional case. Thus, the total mass from rate of the normal component $\dot{M}_n$ is expressed by

$$\dot{M}_n = -\frac{\rho_n A K}{\eta_n}\nabla p. \tag{6}$$

The treatment what follows is quite similar to that by Shotte for the active phase separator [*10, 11* and *12*]. The total mass flow rate $\dot{M}$ should be the sum of the flow rates of both components.

$$\dot{M}=\dot{M}_s+\dot{M}_n=\rho vA=(\rho_n v_n+\rho_s v_s)\,A. \tag{7}$$

Here, v is the mean velocity defined by $v=(\rho_n v_n+\rho_s v_s)/\rho$. The heat is transferred ideally by the normal component. This is described in the following form in the framework moving with the mean velocity v.

$$Q=\rho ST(v_n-v)\,A. \tag{8}$$

On the other hand, the heat is extracted by the evaporating vapor at the downstream side. Thus, Q is related to the latent heat of vaporization, λ, as follows,

$$Q=\lambda\dot{M}. \tag{9}$$

Equating eq. (8) with eq. (9), one has

$$\dot{M}=\rho ST(v_n-v)\,A/\lambda. \tag{10}$$

Substituting eq. (7) into eq. (10), $\dot{M}$ is found to be

$$\dot{M}=(\rho STA\ v_n-ST\dot{M}/\lambda. \tag{11}$$

Then, the total mass flow rate is obtained from eqs. (7) and (11) as

$$\dot{M}=-\frac{\rho ST}{\lambda+ST}\frac{AK}{\eta_n}\nabla p. \tag{12}$$

This gives a theoretical prediction of steady HeII flow through a porous-plug. The total mass flow rate is a strong function not only of the pressure gradient but also of the temperature, because ρ, S, λ and η_n are all strong functions of the temperature. It is of importance to not ethat the functional form indeed looks similar to that for viscous fluids in a sense that the mass flow rate is proportional to the pressure gradient but the proportional constant is much reduced by a factor of ST/(λ+ST), which is found to be at most 0.1. Therefore, the mass flow rate can be properly limited to enough small amount to be evacuated entirely as vapor, that is, no bulk HeII leaks through plugs. Such reduction in $\dot{M}$ is due to the reversal flow of the super component caused by the thermomechanical effect as mentioned before. The dimensions of the experimental porous-plugs given in Table-1 were determined so that they could be used for the zero-g experiment aboard a rocket to be mentioned later. The steady heat dissipation in the HeII vessel was predicted to be at most 200 mW. This figure required the total mass flow rate no more than 10×10^{-6} kg/s. The phase boundary surface might be found

somewhere inside of porous-plugs, ideally at the downstream side, when the phase separation can be accomplished. By a term, phase separation, is meant a state of forming a phase boundary surface inside of a porous-plug, while by leakage as state that bulk liquid phase appears at the downstream side . The upstream side of a plug directly contacts with liquid HeII in the bath in ground experiments, and it may not contact directly with bulk HeII but with saturated film under the zero-g condition in space.

2.2 Experimental Apparatus

The schematic illustration of the experimental apparatus is given in Fig. 3. The apparatus is composed of four parts; the porous-plug section, the helium dewar, the evacuation system for the main helium bath, and the porous-plug evacuation system.

The porous-plug is fixed at the bottom of the evacuation pipe, of which the lowest portion just above the plug mount is made of a glass tube for visual obsevation of the state of the downstream side. It was through this glass tube that it was checked wheter the phase separation is accomplished. This pipe is adjustable in the vertical direction to follow the variation of the liquid level of the main bath.

The temperature of HeII in the helium bath, T_B, was maintained at a constant level with the aid of a pressure regulating valve and a heater immersed in HeII during each series of measurement. The temperature, T_B, was measured by a germanium resistance thermometer, and the pressure by a precision capacitance pressure transducer.

The vapor through a porous-plug was evacuated by a rotary vacuum pump (1500*l*/min), and the flow rate and the pressure at the downstream side of plug were controlled by a control valve. The volumetric flowrate, measured by a rotating flowmeter at the

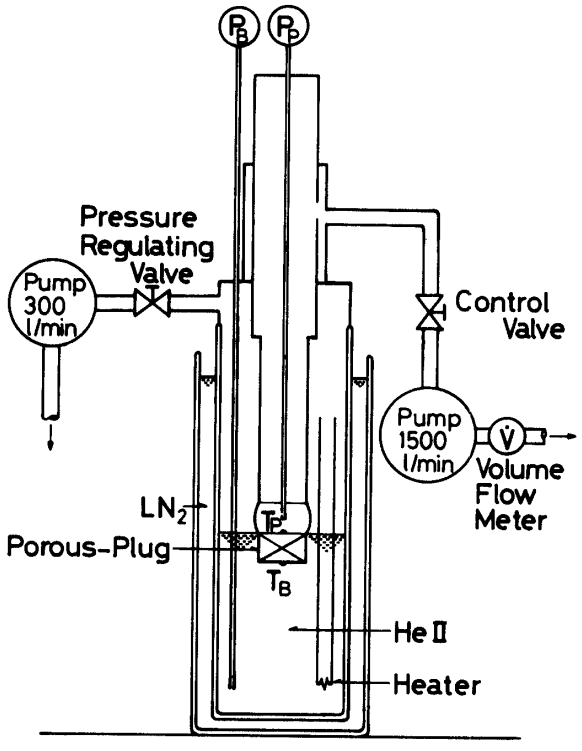

Fig. 3. Schematic illustration of the experimental apparatus; cryostat and two evacuation systems.

exhaust side of the evacuating pump, was converted into the mass flow rate by multiplying it by the density of helium gas under the atmospheric condition. The temperature at the downstream side of the plug was measured by another germanium resistance thermometer, and the pressure at this side was introduced through a static pressure tube to the pressure transducer.

Each thermomeer was excited by 1 μA DC current. The accuracy was within a few mK on the average, though it depended a little on the temperature.

All the data, the mass flow rate $\dot{M}$, the temperatures T_B and T_P at the upstream and the downstream sides of a plug, respectively, the pressures P_B and P_P, and the degree of the ocntrol valve opening were recorded on digital casette magnetic tape for the further data processing by a micro-computer (Panafacom C-15E).

III. Steady Flow Characteristics through Porous-Plugs

The experiments have been carried out firstly in order to investigate the fundamental characteristics of steady flow through porous-plugs in rather systematic ways. Each series of the measurement was taken at a constant T_B while changing the degree of the valve opeing. Experiments were conducted at the temperatures, T_B between about 2.1 K and 1.5 K. The level of porous-plug was adjusted to coincide with the liquid level of bath HeII within $\propto$ mm to avoid undersirable effects of the hydrostatic pressure of HeII by vertically changng the height of the vapor evacuation pipe. The measurements were taken in such a sequence as increasing $\dot{M}$ to the maximum decided by the maximum pumping capability as stepwise opning the control valve and then decreasing it down to nearly zero. The data sampling period was roughly 5 min or loger. Each steady state was confirmed to be established during this period.

3.1 General Flow Characteristics

Typical examples of the data are presented in Figs. 4-a, b and c. These are the experimental results for a ceramic alumina (15 mm-thick) No. 3 (see Table 1) porous-plug at two temperatures, T_B=2.01 K and 1.90 K. Fig. 4-a shows the variation of the mass flow rate $\dot{M}$ with the pressure gradient across the plug, which is defined by

$$\nabla p = \frac{p_B - p_P}{l} . \tag{13}$$

Figs. 4-b and 4-c are the plots of $\dot{M}-\nabla T$ and $\nabla T-\nabla p$ relations, respectively. Here the temperature gradient ∇T is similarly defined by

$$\nabla T = \frac{T_B - T_P}{l} . \tag{14}$$

It is quite obvious from Figs. 4-a and 4-b that there exists a hysteresis feature which appears according to the mode of the flow rate variation, whether it increases or decreases. This hysteresis feature is indicated by arrows in these figures. That is, the

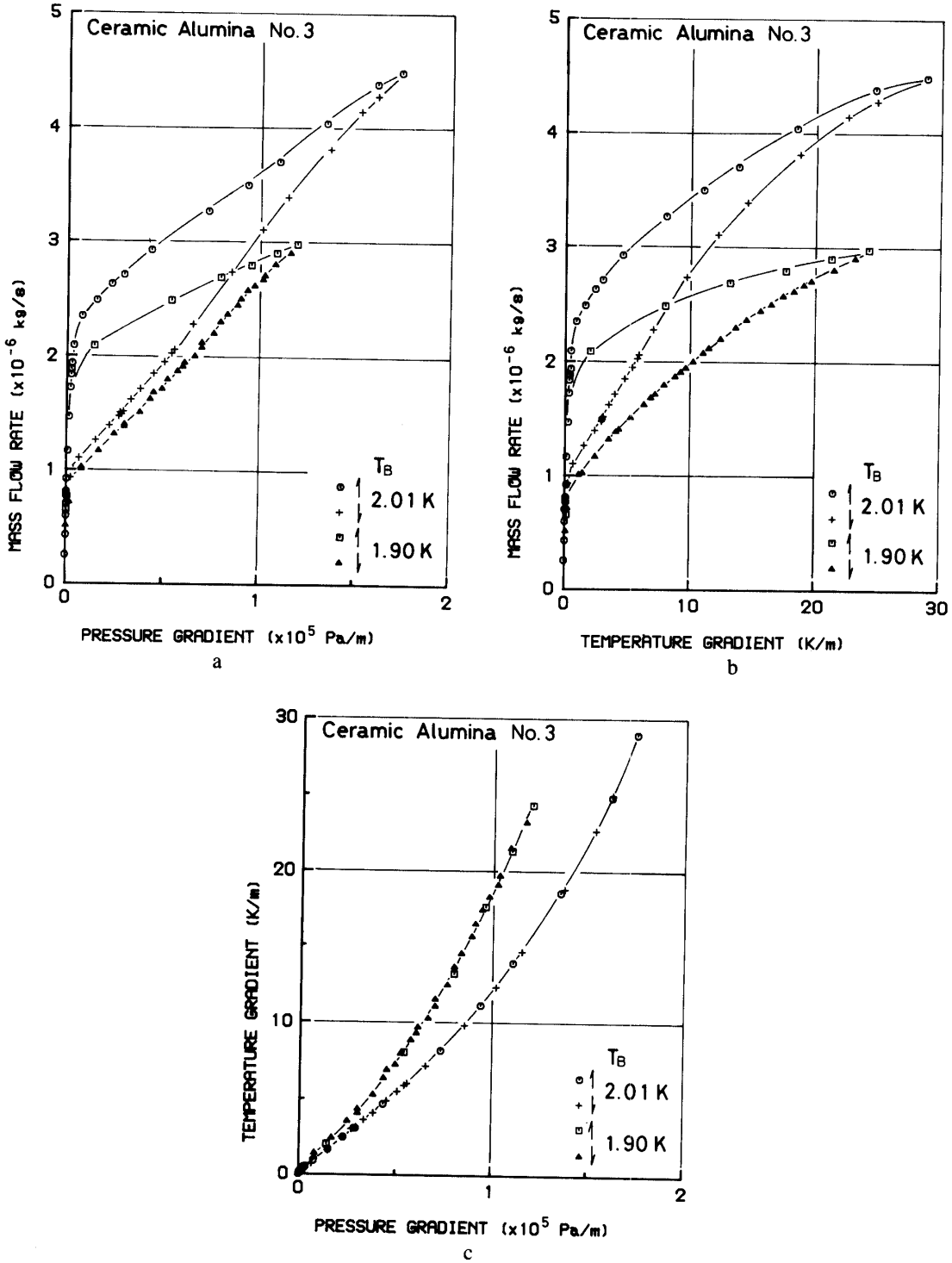

Fig. 4. General steady flow characteristics through No. 3 porous-plug (ceramic alumina), 4-a; $\dot{M}-\nabla p$, 4-b; $\dot{M}-\nabla T$, 4-c; $\nabla T-\nabla p$.

upper branch was observed while $\dot{M}$ increases and the lower while it decreases. However, no hysteresis was recognized in Fig. 4-c, in which $\nabla T - \nabla p$ relation was plotted. A detailed discussion concerning the hysteresis feature will be given in the next section.

It is reasonable to divide the flow situation into four regions: i) The region of non-zero flow while $\nabla p = 0$ (the creeping region); ii) The transition region between the creeping one and the non-linear region where the pressure gradient begins to appear; iii) The non-linear region for larger $\dot{M}$ on the upper branch; iv) The linear region for small $\dot{M}$ on the lower one. In addition, another transition may be recognized between the non-linear region and the linear one. But it is clear that this transition is not essential. The non-linear flow seems to be the only possible situation for very large $\dot{M}$. Thus, the two branches, the linear (lower) and the non-linear (upper), coincide with each other in these cases as seen in Figs. 5 and 6.

The maximum value of ∇p for each case was far smaller than p_B/l, of which value would be presumably reached if an infinitely large pump and a flow passage with zero flow resistance were employed. However, it is obvious that the values of ∇p, and concequently $\dot{M}$, are inevitably bounded smaller than the limiting values because of the finite capability of the pump and the non-zero flow resistance of the vapor passage.

Similar results are presented in Figs. 5 and 6 for a ceramic alumina (No. 4) and a sintered stainless steel porous-plugs, respectively. It is seen from these that the flow characteristics quantitatively varies with the kinds of porous-plugs. This feature is clearly shown in Fig. 7, where the variations of the mass flow rate with the pressure gradient (only of the lower branch) are compared among four kinds of porous-plugs at a temperature, 1.9 K. Note thath the mass flow rate $\dot{M}$ is normalized by the cross sectional area for the sake of comparison in this figure. It is also clear that the flow

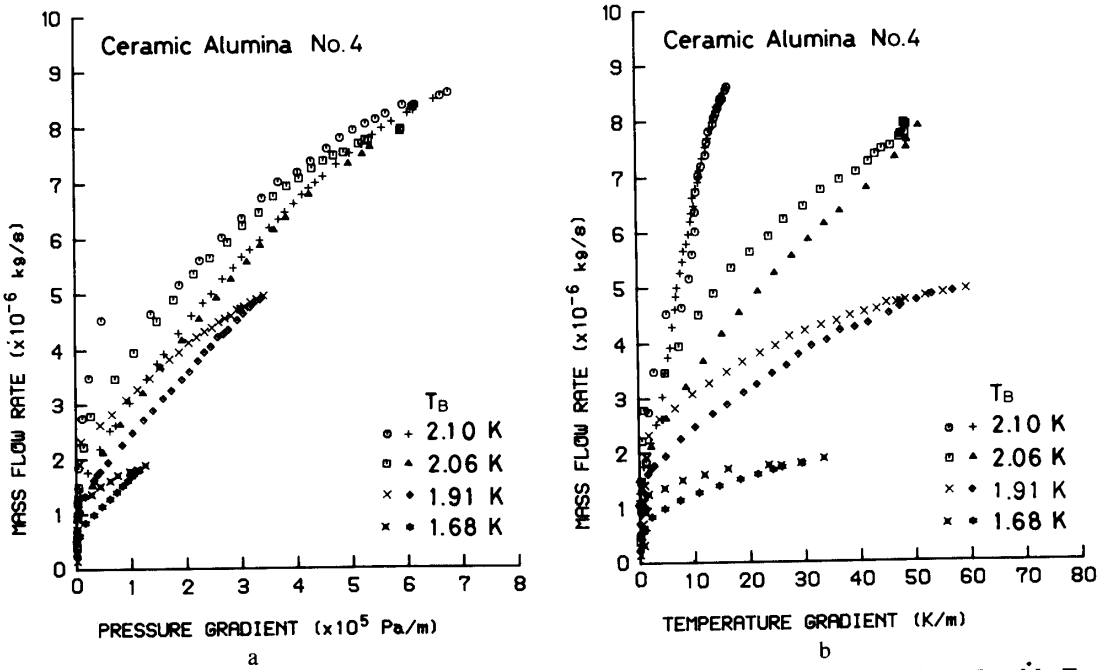

Fig. 5. General steady flow characteristics through No. 4 porous-plug (ceramic alumina), 5-a; $\dot{M} - \nabla p$, 5-b; $\dot{M} - \nabla T$.

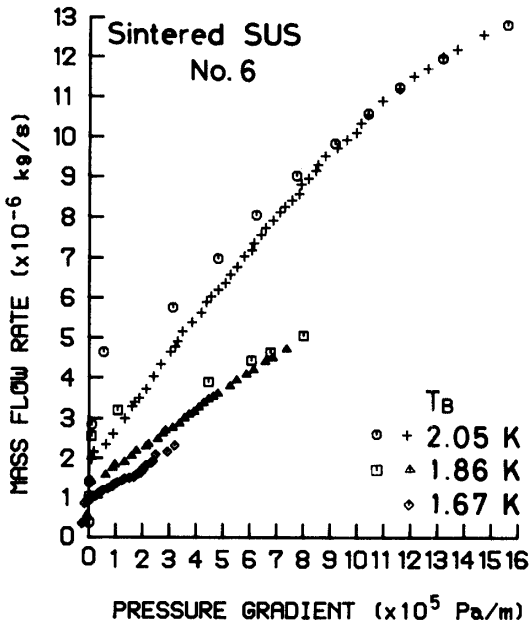

Fig. 6. General steady flow characteristics through No. 6 porous-plug (ceramic alumina).

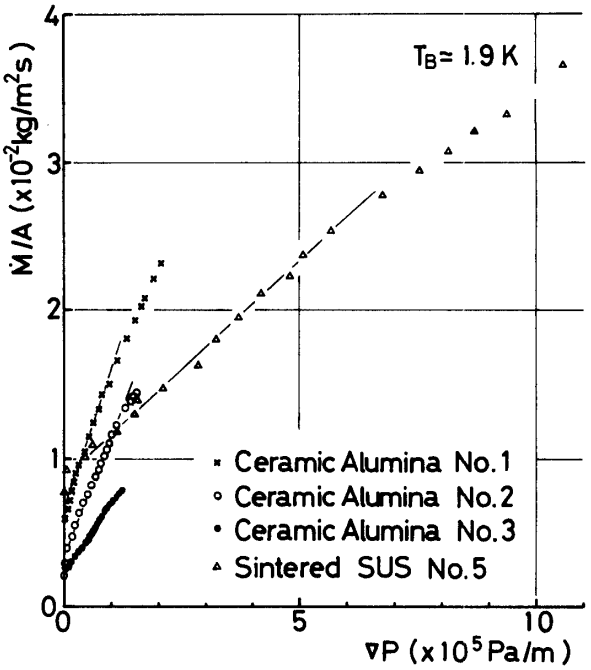

Fig. 7. Comparison of flow characteristics for four types of porous-plugs at T_B=1.9 K. The mass flow rates are normalized by the cross sectional area, A.

conductance considerably differs among plugs as anticipated by their large variation in the permeability. This will be referred to in more detail in the section 3.5

The effect of the bath temperature, T_B, is shown in Figs. 8-a and 8-b for the ceramic clumina (10 mm-thick) No. 2 porous-plug, where only the lower branches are presented for simplicity. It is seen that the ranges of variations in ∇p and $\dot{M}$ become wide and the

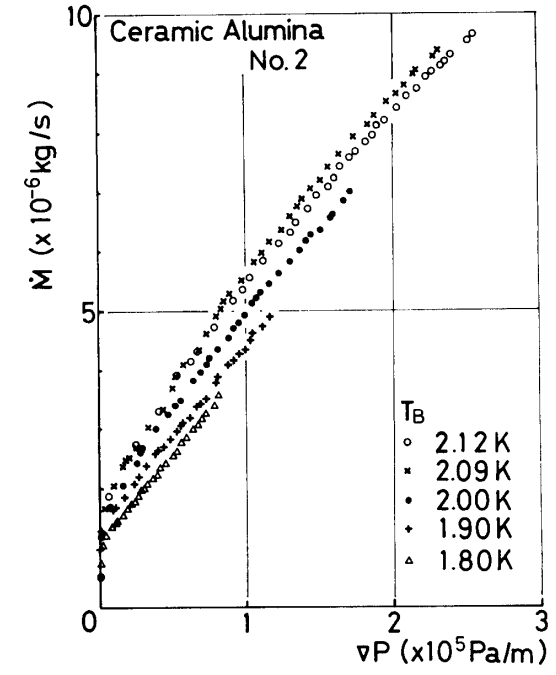

a

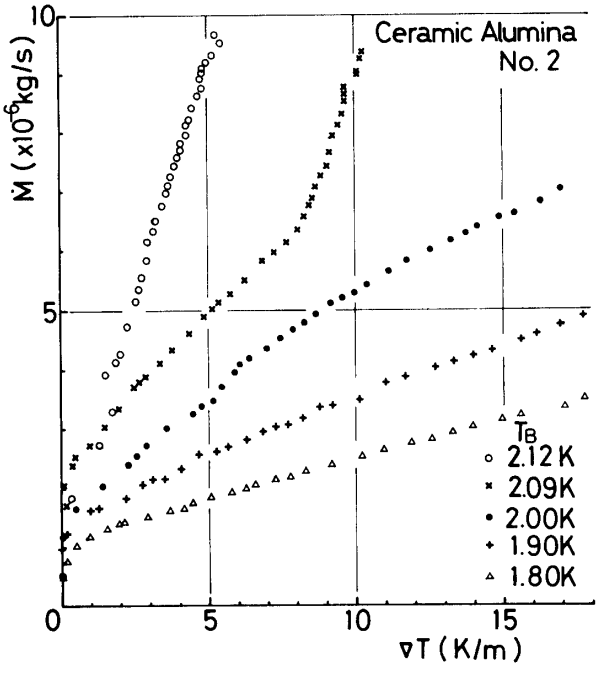

b

Fig. 8. Variation of flow characteristics with bath temperature T_B (lower branch only): Ceramic alumina (No. 2) porous-plug. 8-a; $\dot{M}-\nabla p$, 8-b; $\dot{M}-\nabla T$.

magnitude of $\dot{M}$ does large for a given value of ∇p, as the temperature rises. The flow conductance through each plug, which is equivalent to the gradient of the data points, only weakly depends on the temperature. It is of interest to note on the $\dot{M}-\nabla T$ plot in Fig. 8-b that a radical change in the flow state might appear for large $\dot{M}$ at higher temperatures, 2.12 K and 2.09 K, though no such variations are recognized on the $\dot{M}-\nabla p$

diagram in Fig. 8-a. This peculiar behavior appeared only for large $\dot{M}$ at T_B=2.09 K, but it did even for small $\dot{M}$ at T_B= 2.12 K. This behavior should be considered as a typical flow feature of some particular porous-plugs for large M at higher temperatures, because it was also observed for the other porous-plugs such as the ceramic alumina (5 mm-thick) No. 4.

The relation between the temperature T_P and the pressure P_P at the downstream side of a porous-plug is given in Fig. 9, where the curve of saturated vapor pressure of HeII is also drawn for comparison. These data were obtained just in the same experiments as given in Figs. 8-a and 8-b. This figure demonstrates that the porous-plug performed a perfect vapor-liquid phase separation, that is, no leakage of liquid HeII through the porous-plug, because all data points are plotted below the saturated vapor pressure line. Only one point just on the curve for each temperature serns to represent the whole data points in the creeping region. It is also clear from this fiture that the peculiar behavior described in the last paragraph, by no means resulted from leakage of liquid HeII. It is confirmed that the pressure at the downstream side of porous-plug was always lower than the saturated vapor pressure for any kinds of porous-plugs tested except that the flow state was in the creeping region. The deviation of p_P from the curve tends to get small as the temperature T_B drops.

Similar results to us were presented by Hendricks *et al.*[7], one of which is reproduced in Fig. 10 for reference. They tested a sintered stainless steel porous-plug of 0.5-μm mean pore diameter. It seems that the flow characteristics is rather similar to the present ones, though experimental details are not quite clear.

Another series of experiment was also conducted, in which the temperature T_B was changed while the condition of the vapor flow passage, that is, the valve opening, was kept unchanged. It is thought that this situation may be rather common to onboard applications with such passive phase separators as porous-plugs. The results are presented in Fig. 11, in which the opening of the control valve was indicated by "1/4 open" or "1/2 open". It is seen that the mass flow rate considerbly changes with the

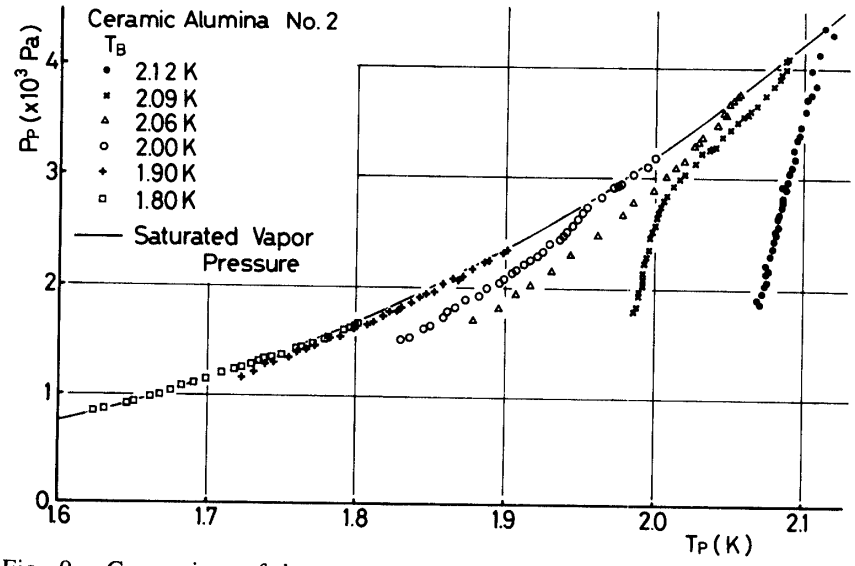

Fig. 9. Comparison of the vapor state at the downstream side of porous-plug (T_P, p_P) with the saturated vapor state: Ceramic alumina (No. 2) porous-plug.

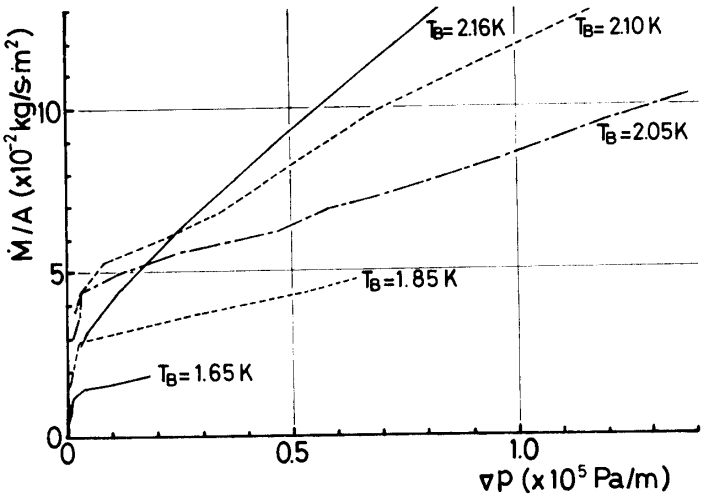

Fig. 10. Steady flow characteristics through a 1/4"-thick stainless steel porous-plug with .5 μm mean pore diameter [7].

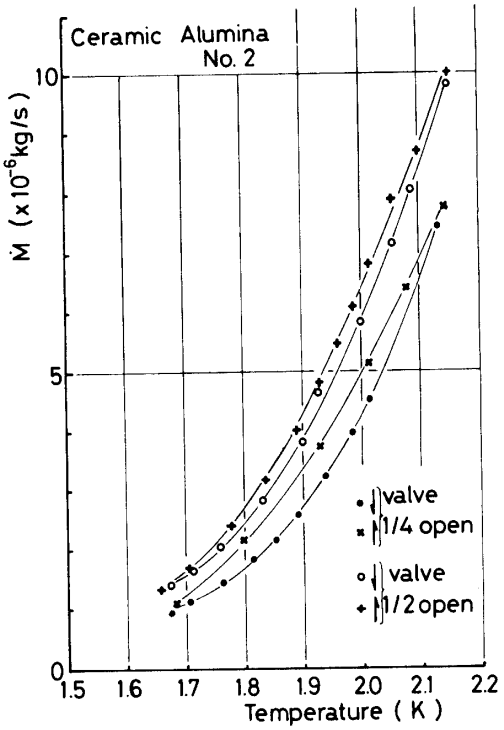

Fig. 11. Variation of mass flow rate with T_B at a fixed vapor flow condition. "1/2 open" stands for a valve condition in which the valve orifice is half open.

temperature T_B, even when the flow congfiguration was kept unchanged, and that hysteresis also appears under such a situation.

3.2 Hysteresis of Flow

An experiment was attempted to investigate the hysteresis of flow in more detail, of which results are given in Figs. 12-a, b and c. The opening of the control valve was

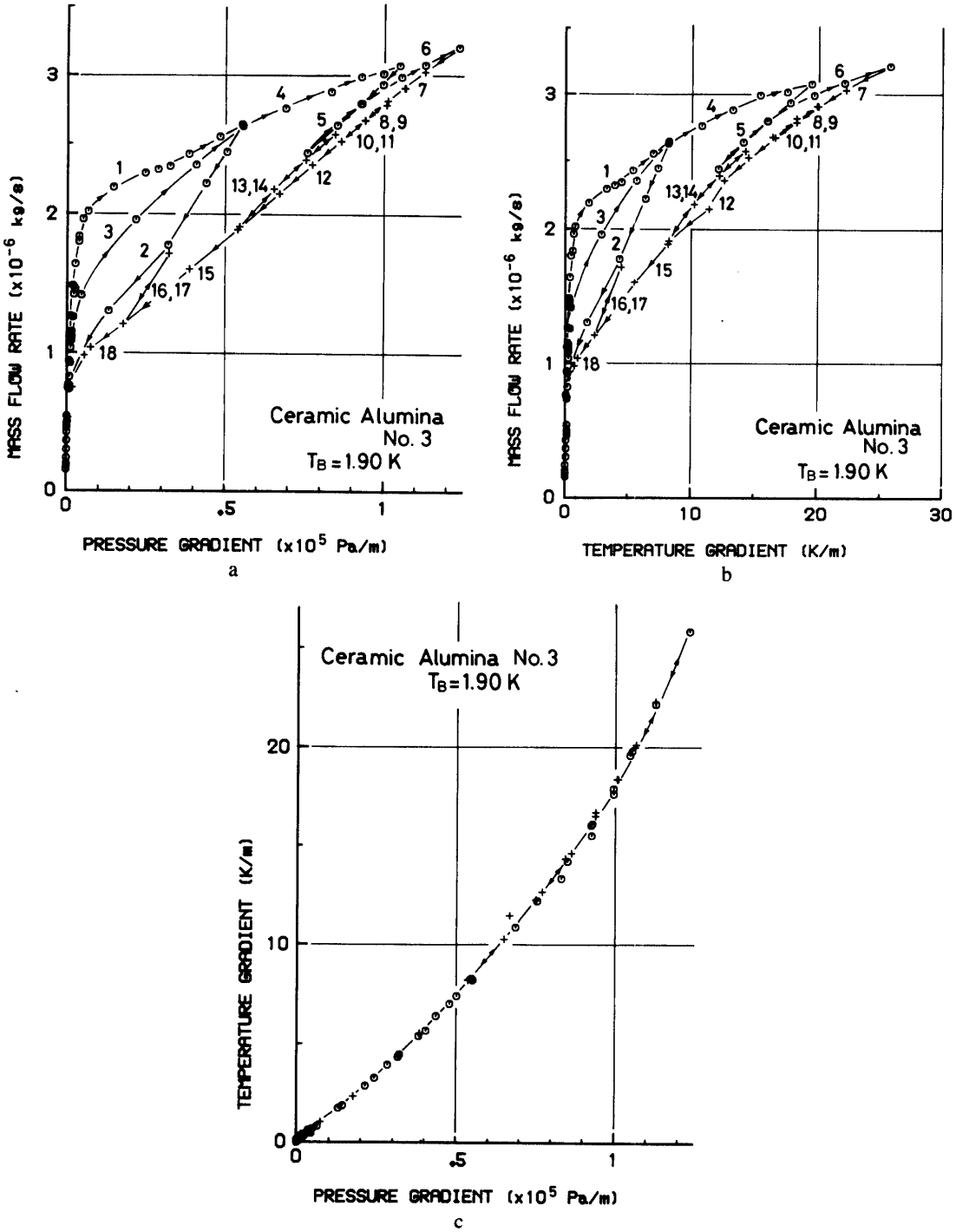

Fig. 12. Detailed examination of hysteresis behavior. The flow rate was varied in zigzag manners such as from the process 1 through process 18. 12-a; $\dot{M}-\nabla p$, 12-b; $\dot{M}-\nabla T$, 12-c; $\nabla T-\nabla p$.

varied in a zigzag manner, as indicated by arrows 1 through 18 in the figures, instead of changing it monotonously as in the previous cases. Each data was taken after a steady state was attained. The time interval of the data sampling was about 5 min or longer. The experiment started at a condition of very small $\dot{M}$, and then it was stepwise increased (process 1 as indicated in Fig. 12-a). Then, the variation of the valve opening was reversed at a condition of $\dot{M}=2.6\times10^{-6}$ kg/s ($\nabla p=0.55\times10^{5}$ Pa/m) down to the creeping region where $\nabla p=0$ (process 2). The valve opening was again stepwise increased and the same flow condition was reached (process 3) at $\dot{M}=2.6\times10^{-6}$ kg/s, though the process to this condition did not exactly follow the previous one (process 1). The experiment was conducted in such a manner as indicated by the process 1 through 18 in the figure. Several experimental facts can be pointed out from the results: i) all the data points lie on or between the upper and the lower branches. ii) When the mass flow rate was being increased starting from the creeping region (processes 1 and 3) or from a state of very small $\dot{M}$ (process 16), the flow state varied toward the upper branch. However, the processes were not reproducible in the transition region between the creeping and the non-linear ones (processes 1 and 3). iii) When $\dot{M}$ was being decreased from a state on the upper branch (processes 2 and 5), the flow state tended toward the lower branch. In fact, when $\dot{M}$ was enough large at the starting state, a state on the lower was actually reached (process 5). iv) The flow state varied just on the lower branch irrespective as to whether $\dot{M}$ was increased or decreased (processes 8→9, 10→11 and 13→14). All these features are also seen in the $\dot{M}-\nabla T$ plot given in Fig. 12-b. It is of interest to note that all the data points lay on a single curve of the $\nabla T-\nabla p$ plot shown in Fig. 12-c. It seems that there exists a unique relation between the pressure difference p_B-p_P and the temperature difference T_B-T_P or between p_P and T_P independent of $\dot{M}$. In this particular case, the relation was found to be that of saturated vapor. However, such a unique relaiton was also observed in cases away from the saturation condition. One possible explanation may be given by the Joule-Thomson effect occurring primarily related to the vapor flow in porous-plugs. This will be discussed in more detail later. The hysteresis may be caused by the configuration of the vapor-liquid phase boundary inside of the porous-plug. The porous-plug must be completely saturated with HeII in the creeping region, while the downstream portion of it must at least be dried out for larger $\dot{M}$. This can be confirmed by comparing p_P with the saturated vapor pressure given in Fig. 9. On the other hand, the pore diameter of each porous-plug was widely distributed as mentioned previously. Thus, the average location of the phase boundary and the configuration of wetting are not reversible but depend on whether $\dot{M}$ is being increased or deceased. In addition, the hysteresis character of adsorbed thin film of HeII in local fine pores in porous matrices might appear in connection with its development and extinction. For enough large $\dot{M}$, any distinctions between the upper and the lower branches dissapear, and the flow characteristics is just non-linear. There can not be hysteresis in these cases. It is also an experimental consequence that the upper branch is more or less metastable, while the lower one are stable.

3.3 Flow in the Creeping Region

Results of experiments to investigate the flow in the creeping region and of very small

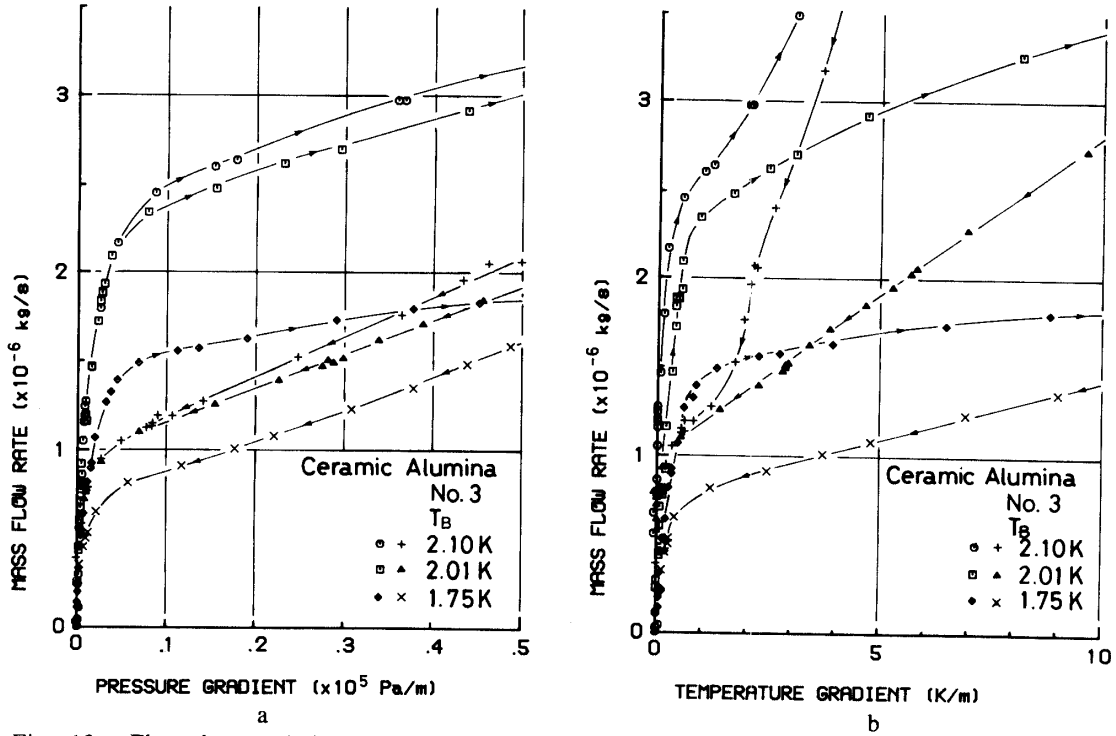

Fig. 13. Flow characteristics; the creeping region and the occurrence of ∇p 13-a; $M-\nabla p$, 13-b; $M-\nabla T$.

pressure gradient ∇p are presented in Figs. 13-a and 13-b, which may be regarded as close-ups of Figs. 4-a and 4-b, respectively, for small values of ∇p and ∇T. It can be concluded within the experimental error that a number of data points are just on the ordinate. This fact means that the mass flow rate is not zero even if both the pressure and the temperature gradients are equal to zero. It seems that the super component can alone flow through the porous-plug due to the thermomechanical effect caused by a heat leak to plugs. In fact, it was usually observed through the glass tube that bulk HeII slowly leaked out through a plug when the control valve for the vapor evacuation was completely closed. A part of the heat is consumed for HeII to evaporate, and the rest is given to the super component which flows out through the plug with zero-entropy. The flow ate $\dot{M}$ is controlled by the opening of the vapor evacuation valve. As the vapor flow rate becomes large, it happens that the evaporated mass can not be compensated fully by the super componnet. Thus, the normal component begins to flow to develop the gradients of the pressure and the temperature. Their developments are only a little for small $\dot{M}$. However, their increasing rates with respect to $\dot{M}$ become drastically large as $\dot{M}$ exceeds a certain value. The upper limit of $\dot{M}$ in the creeping region, $\dot{M}_0$, which is determined as $\dot{M}$ at the point where the extraporated line of the linear branch cuts the ordinate, is plotted against T_B in Fig. 14. It is seen that $\dot{M}_0$ tends to increase with the temperature, T_B. It should be added that it is experimentally verified that $\dot{M}_0$ is increased by adding heat to the downstream side of a plug. This will be discussed in the next chapter. Effective phase separation action can be exerted only when ∇p and ∇T are developed across plugs. Therefore, it should be emphasized that it is difficult to perform the phase separation for so small $\dot{M}$ that the flow may be in the creeping region.

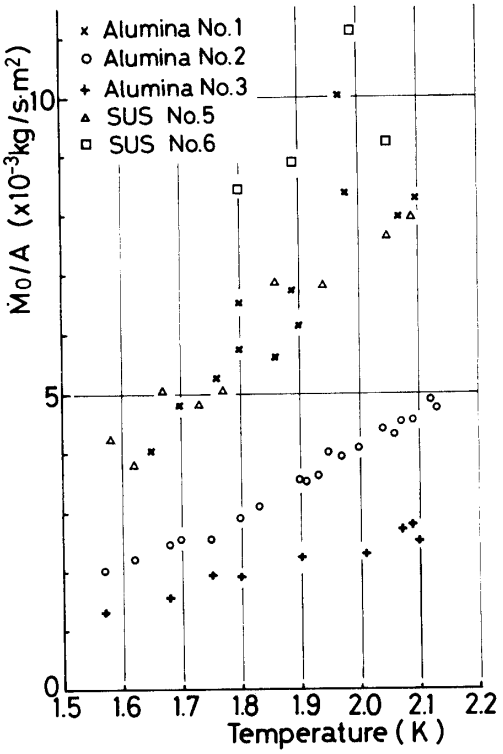

Fig. 14. Variation of the maximum creeping flow rate, $\dot{M}_0$, with T_B for several porous-plugs.

3.4 Non-Linear Flow Region

As described in the previous sections, the mass flow rate increases non-linearly with the presure gradient and with the temperature gradient for large values of $\dot{M}$, and the distinction between the upper and the lower branches disappears for enough large $\dot{M}$. However, such unique curve was actually observed only when the evacuation system has enough capability for the volume flow rate. In many cases, the end part of the lower branch for larger $\dot{M}$ just shows a transition between the non-linear and the linear regions. Thus, the non-linear flow region was recognized primarily on the upper branch for lage values of $\dot{M}$ and sometimes on the lower branch.

The data are plotted on full-logarithm graphs in the form $\dot{M}$-$\dot{M}_0$ vs ∇p relation in Figs. 15-a and b and Fig. 16 to examine the functional relation between the two variables in the non-linear region. The quantity $\dot{M}_0$ is the maximum flow rate in the creeping region as define before,which contributes neither to ∇p nor to ∇T. Solid lines in these figures indicate a slope with a gradient of 1/2. It is clear from these that the data points in the non-linear region lie on the lines independently of the temperature T_B. This fact is also valid for any porous-plugs. Therefore, it is experimentally proved that the 1/2-power law is essential to the relation, that is;

$$\dot{M}-\dot{M}_0=\alpha(\nabla p)^{1/2}, \tag{15}$$

where α is a constant to be investigated, which may vary with T_B and the kind of

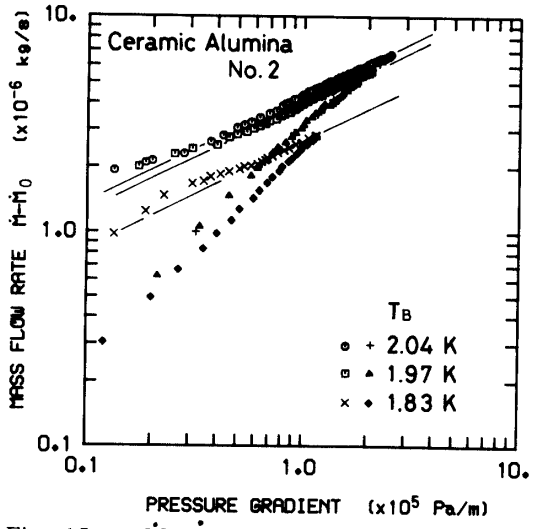

Fig. 15-a. $\dot{M}-\dot{M}_0$ vs ∇p relation for the ceramic alumina No. 2 porous-plug. Solid lines are eye guides with a gradient of 1/2.

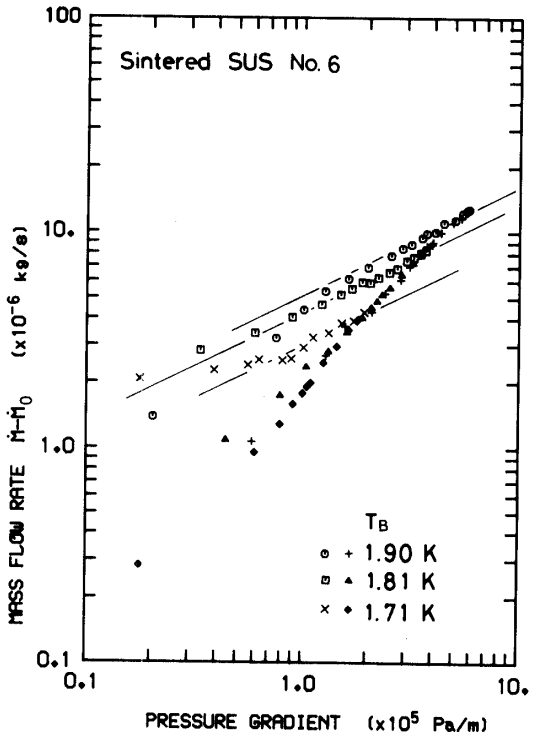

Fig. 15-b. $\dot{M}-\dot{M}_0$ vs ∇p relation for the SUS No. 6 porous-plug. Solid lines are eye guides with a gradient of 1/2.

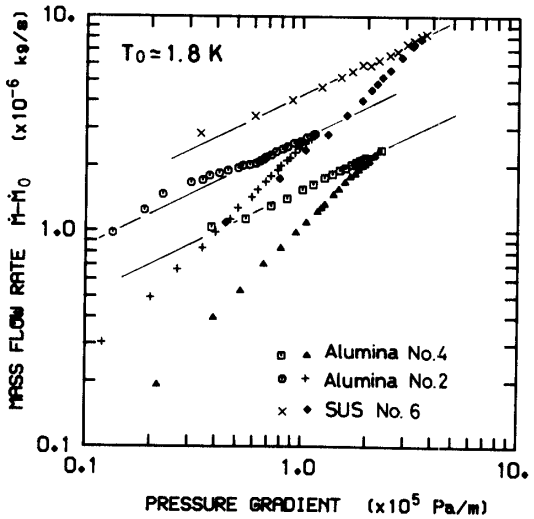

Fig. 16. $\dot{M}-\dot{M}_0$ vs ∇p relation for several porous-plugs. Solid lines are eye guides with a gradient of 1/2.

porous-plug. The result is presented in Fig. 17-a. It is quite reasonable to consider that α is proportional to the cross sectional area, A. The dimensional analysis suggests that α should be proportional to $\sqrt[4]{k}$ and $\sqrt{\rho_v}$ as well as to A, provided that the major pressure drop is caused by the vapor flow through a porous-plug. Here, the density of the vapor, ρ_v, may be replaced by that of the saturated vapor, ρ_{sat}, for simplicity. Thus, one can get

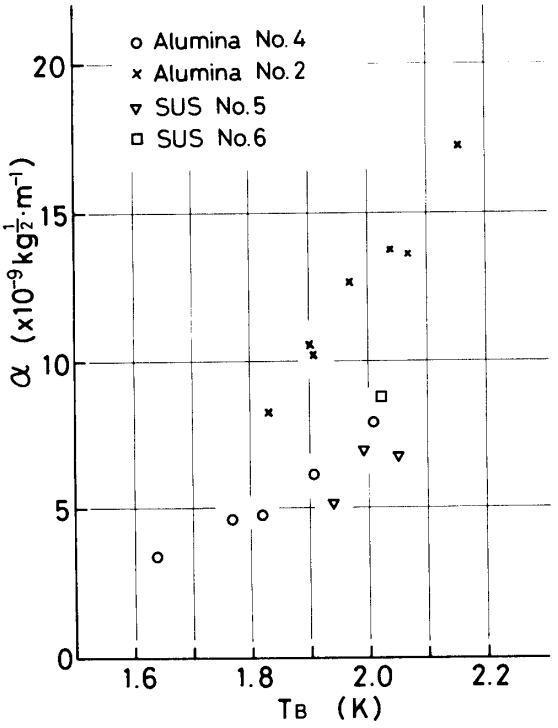

Fig. 17-a. Variation of the coefficient α with T_B in the non-linear region for a number of porous-plugs: $\dot{M}-\dot{M}_0=\alpha(\Delta p)^{1/2}$.

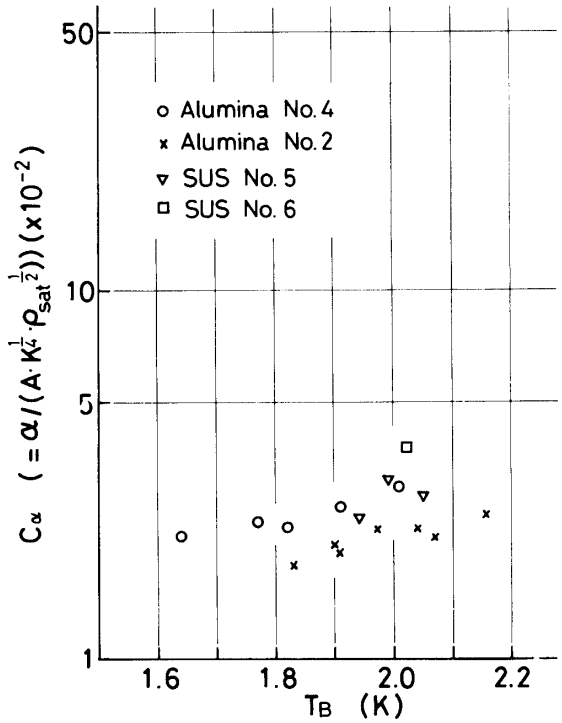

Fig. 17-b. Universal constant C_α obtained from the experimental results given in Fig. 17-a: $\dot{M}-\dot{M}_0=C_\alpha A K^{1/4}\rho_{sat}^{1/2}\nabla p^{1/2}$.

a following expression for α;

$$\alpha = c_\alpha A^4 \sqrt{K} \sqrt{\rho_{sat}}, \tag{16}$$

where, C_α is a universal constant. The result is plotted against T_B in Fig. 17-b. It may be considered that the coefficient C_α only weakly depends on the temperature, T_B, and is almost independent of the kind of porous-plugs. This seems to indicate that the functional relation, Eq. (16), is a unique one in the non-linear flow region. It is of interest to note that the kinematic viscosity of vapor, η_v, is not included in the expression. In other words, the flow resistance is independent of η_v, consequently, of the Reynolds number. It is well known that such situation is observed in flows through rough pipes for considerably large Reynolds numbers [*14* and *16*]. A porous medium may be regarded as an aggregation of rough pipes. Therefore, it is quite natural to conclude that the total pressure drop in a porous-plug is contributed primarily by the vapor flow, which is rather turbulentlike.

The relation between $\dot{M}-\dot{M}_0$ and ∇T is also examined in the similar manner to the last one. Some examples of the results are redrawn in full-logarithmic graphs in Figs. 18-a and -b, where solid lines are eye-guides with a gradient of 1/3. The exponent, n_β, of the power law such as

$$\dot{M}-\dot{M}_0=\beta(\nabla T)^{n_\beta} \tag{17}$$

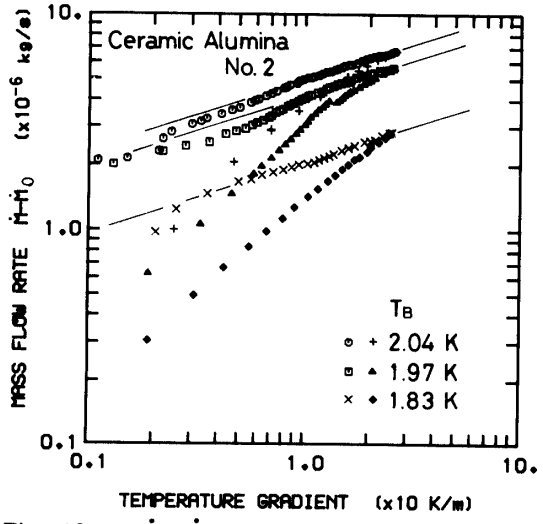

Fig. 18-a. $\dot{M}-\dot{M}_0$ vs ∇T relation for the ceramic alumina No. 2 porous-plug. Solid lines are eye guides with a gradient 1/3.

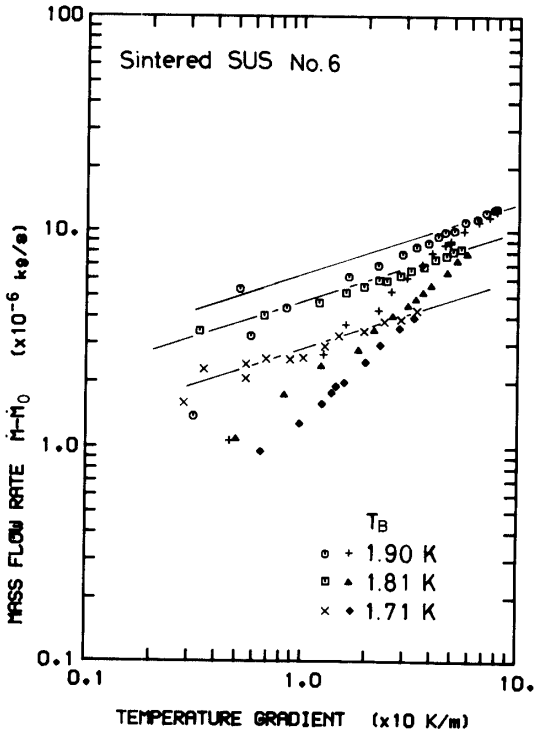

Fig. 18-b. $\dot{M}-\dot{M}_0$ vs ∇T relation for the SUS No. 6 porous-plug. Solid lines are eye guides with a gradient 1/3.

is checked for various temperatures and porous-plugs. It is found that the value of the exponent scatters between 1/2 and 1/3 and that there is a clear distinction in the functional relation betweeen ceramic alumina porous-plugs and SUS plugs. That is to say, the functional ralation between $\dot{M}-\dot{M}_0$ and ∇T is not so clear as $\dot{M}-\dot{M}_0$ vs ∇p relation.

Relations between ∇p and ∇T are presented in Figs. 4-c and 19. It is hard to find any clear hysteresis feature in these figures. Therefore, it can be tentatively concluded that there is a unique relation between ∇p and ∇T, which is independent of $\dot{M}$. In other words, there is a unique relation between the pressure and the temperature at the downstream side of a porous-plug, since the pressure, p_B, and the temperature, T_B, at the upstream side were kept unchanged during a series of experiment. The hysteresis must be caused by the irreversible feature of the vapor-liquid phase surface in a porous material, as mentioned previously. One of the plausible effect which governs such unique relation between the pressure and the temperature and is independent of the mass flow rate is the Joule-Thomson one. A very rough estimation gives a temperature drop of order of 100 mK, though accurate calculation can not be performed because no accurate thermophysical property values are available in these conditions. This order of magnitude of the crude estimate agrees with experimental values.

In Fig. 19, London's relation

$$\Delta p=\rho s\Delta T \tag{18}$$

is also plotted by a solid line. It is obvious that the ratio $(T_B-T_p)/(p_B-p_p)$ of the present

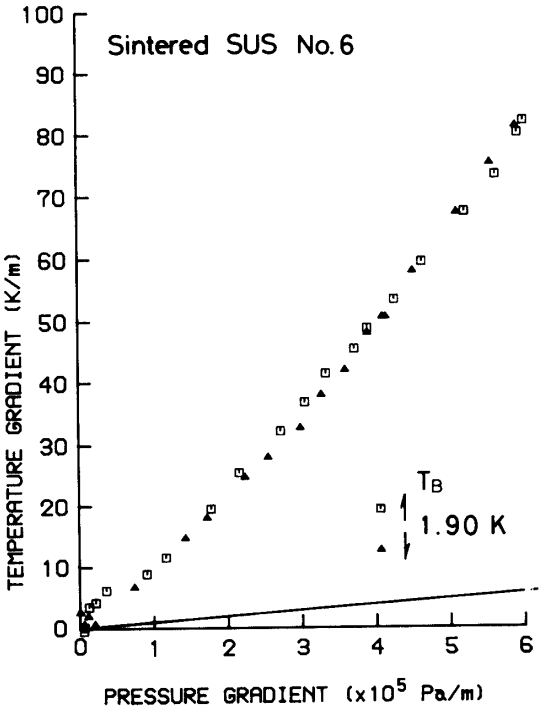

Fig. 19. ∇T vs ∇p relation of SUS No. 6 porous-plug. The solid line is the London equation (18).

result is far larger than the prediction $1/(\rho s)$. It is one of the remarkable feature of a porous-plug that the overall temperature drop across a plug is considerably large. This may be regarded as another evidence that the flow phenomena of HeII through a porous-plug in the non-linear region takes place by no means on the ideal level.

The flow characteristics for the case of large $\dot{M}$ can be summarized as follows. There exist both large pressure and temperature drops across plugs and the functional dependences of the two on the mass flow rate are of non-linear. Liquid HeII occupies just an upstream portion of plug and the rest is done by its vapor. This vapor flow dominates such flow characteristics as large pressure and temperature drops. The flow must be highly turbulentlike.

3.5 Linear Flow Region

It has experimentally confirmed that the mass flow rate changed linearly with the pressure gradient when the flow situation was varied along the lower characteristic branch. This situation is followed by the creeping region for smaller $\dot{M}$. However, such a linear relation can by no means be recognized in the $\dot{M}-\nabla T$ relation as seen from Fig. 4-b. This feature is quite common to any porous-plugs as shown in Figs. 5-a, -b, 6, 7, 8-a and -b. It is considered that the overall temperature drop is predominantly determined by the pressure drop independently of the mass flow rate. It is well known that such phenomena are caused, for example, by the Joule-Thomson effect. This independent feature of $\dot{M}$ is demonstrated by an experimental fact that no hystereses are recognized

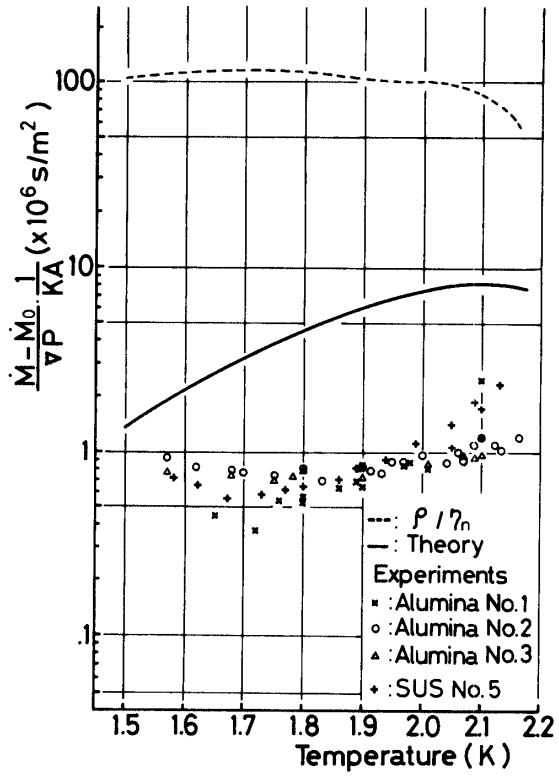

Fig. 20. Variation of flow factor with T_B. ——; theory ($\rho ST/(\lambda+ST)\eta_n$, Eq. (12)), ------; ordinary viscous fluid (ρ/η_n, Eq. (19)).

provided that the temperature gradient is plotted against the pressure gradient as in Figs. 4-c, 12-c and 19. Quantitative variations of the flow characteristics for several kinds of porous-plugs in this region at a temperature are seen in Fig. 7. Such variation may be a natural reflection of the differences, above all, in the magnitude of the permeability and $\dot{M}_0$. The dependence of the flow characteristics on the tempearture, T_B, is shown in Fig. 8-a for the No. 2 porous-plug. It is seen from this that the overall flow conductance, which is equivalent to $(\dot{M}-\dot{M}_0)/\nabla p$, is a weak function of the temperature, T_B.

It is considered that this linear region may correspond to cases treated by the theory given in section 2.1. The values of $(\dot{M}-\dot{M}_0)/(\nabla pKA)$ calculated from the linear portion are plotted against the temperature for each porous-plug in Fig. 20 together with the theoretical prediction. Also by a dotted line is given the estimated value which would be expected if the liquid was assumed to be just a viscous fluid with the viscosity η_n and the density ρ; that is

$$M=\frac{\rho AK}{\eta_n}\nabla p. \tag{19}$$

It is of interest to find by comparing the two curves that the flow conductance across a porous-plug is remarkably reduced by taking the thermomechanical effect of the superfluid into account. This effect gets extremely large for lower temperatures. It is this effect that prevents the liquid HeII from leaking out through porous-plugs. The agreement between the experimental data and the theoretical curve (solid line) is generally poor, though it seems to get better at lower temperatures. However, the result shows that all the data exhibit a very weak dependence on the temperature for any porous-plugs. The discrepancy between the experimental value and the theory seems to suggest that the basic assumption that the liquid-vapor phase boundary should be located at the downstreammost of a plug is unrealistic. The real phase boundary must be located somewhere inside of a plug. In this situation, the pressure drop would be contributed from both flows of the liquid HeII and the vapor. Therefore, a quantity $(p_B-p_I)/x$ should be regarded as the true pressure gradient in the liquid HeII phase instead of $(p_B-p_P)/l$, where p_I and x are the pressure at the liquid-vapor phase boundary and its location measured from the upstream side of a porous-plug, respectively. This can be explicitly formulated as follows;

$$\begin{aligned}\dot{M}-\dot{M}_0&=\frac{\rho ST}{\lambda+ST}\frac{AK}{\eta_n}\frac{p_B-p_I}{x} && \text{(in liquid HeII)}\\ &=\frac{\rho_v AK}{\eta_v}\frac{p_I-p_P}{l-x}, && \text{(in vapor)}\end{aligned} \tag{20}$$

where ρ_v and η_v are the density and the visocosity of the vapor, respectively. This results in

$$\dot{M}-\dot{M}_0=\frac{\alpha_v\alpha_I l}{\alpha_I l+(\alpha_v-\alpha_I)x}\frac{p_B-p_P}{l}, \tag{21}$$

Here we have

$$\alpha_v=\frac{\rho_v AK}{\eta_v}$$

$$\alpha_l=\frac{ST}{\lambda+ST}\frac{\rho AK}{\eta_n}$$

A rough estimate indicates that the flow factor α_v for the vapor is smaller than α_l for the liquid HeII. Eq. (21) suggests that $\dot{M}-\dot{M}_0$ is not exactly linear to $(p_B-p_P)/l$ as x may vary with $\dot{M}$. However, such non-linear feature may be considered to be weak, because the variation of x can not be so large in the linear region. A result derived from the above discussion is that

$$\frac{p_B-p_l}{x}<\frac{p_B-p_P}{l}<\frac{p_l-p_P}{l-x} \tag{22}$$

Therefore, the agreement between the experiments and the theory should be much improved by taking $(p_B-p_l)/x$ for the pressure gradient in the liquid HeII phase. Unfortunately, no experimental data giving p_l and x are available so far. This tentative conclusion is compatible with the fact that the agreement gets better for lower temperatures. α_v may be much close to α_l or x may be nearly equal to l at these temperatures. The latter case is more likely to occur. Thus, the flow situation at these low temperatures may be rather ideal as treated by the theory.

It should be pointed out that the temperature drop, T_B-T_l in the liquid phase predicted by the theory is

$$T_B-T_l=(P_B-p_l)/\rho S, \tag{23}$$

which is nothing but an estimate by the London equation (18). The experimental overall temperature drop has been found to be far larger than the estimate by almost two orders of magnitude. This may imply that the temperature drop occurring in the vapor flow is extremely larger than that in the liquid HeII. It is an explanation to such excess temperature drop that the Joule-Thomson effect dominates in the vapor flow through the plug. Of course, it may be another plausible interpretation that the liquid HeII flow through a porous-plug is in the breakdown state, that is, in the superfluid turbulent state. Further experiments are required to clearify the origin of the excess temperature drop.

3.6 Bulk HeII Leakage through Porous-Plugs

The term "leak" is loosely defined as a state in which bulk HeII appears at the downstream side of porous-plugs. It is natural to consider that the downstream side of a porous-plug is covered with absorbed thin film though it may sometimes be unsaturated film. However, in the leak state, bulk HeII is observed there, sometimes in a state of puddle or sometimes in a manner of intermittent spouts. In addition, when the

evacuation line coming from a porous-plug was closed, HeII puddle was always recognized. We exclude this particular state from the present discussion because porous-plugs are not activated in this situation. In fact, such a puddle was observed to be gradually sucked into a plug, when the evacuation line was opned to the vacuum pump, or when the upstream side of plug was heated to rise the temperature of HeII in the

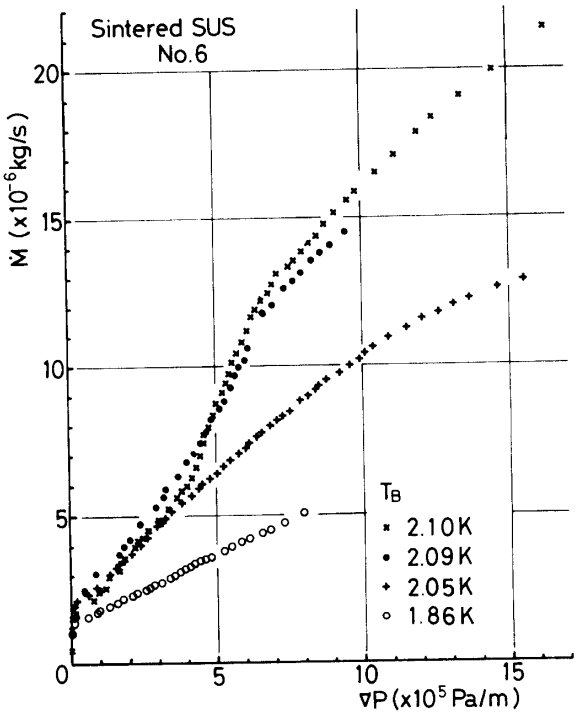

a

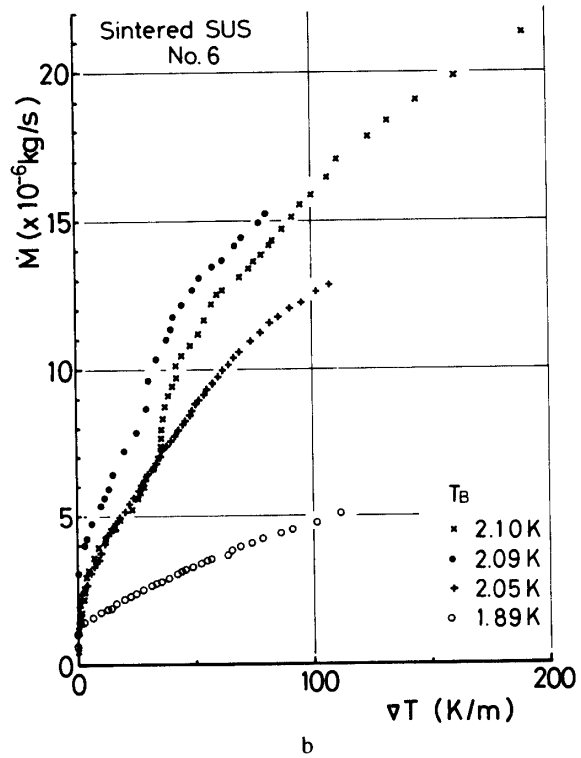

b

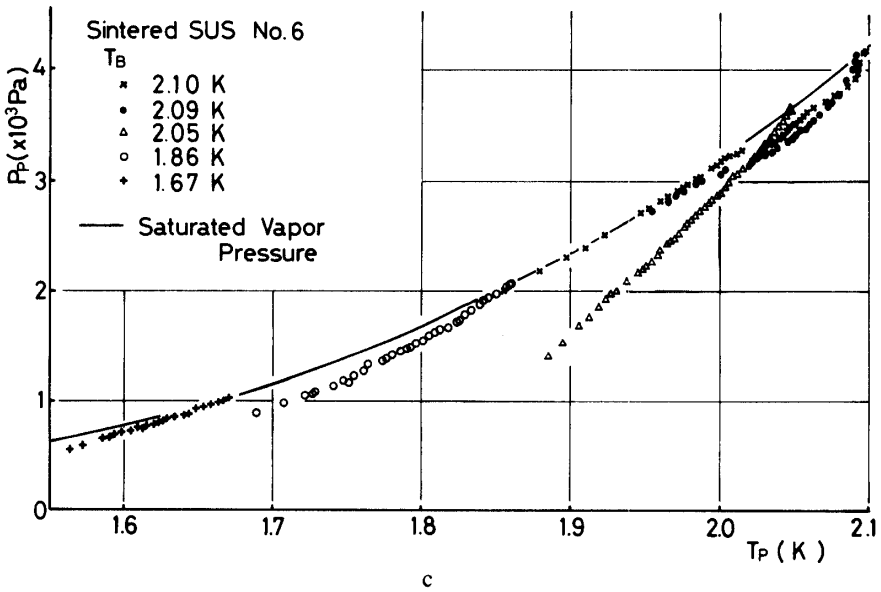

c

Fig. 21. Steady flow characteristics through No. 5 porous-plug (SUS). Special attention should be paid to the leak state at higher temperatures (T_B>2.06 K). 21-a; M−Δp, 21-b; M−ΔT, 21-c; p_P−T_P.

bath.

An example of the flow characteristics including the leak state is seen in Figs. 21-a, b and c for a sintered SUS porous-plug. Intermittent spouts of HeII were observed atT_B>2.06 K. It is obvious that the flow characteristics at themperatures below 2.05 K are basically similar to those of other porous-plugs in the normal operation. However, the growth rate of $\dot{M}$ with respect both to the pressure gradient and to the temperature gradient became larger for larger $\dot{M}$ at the temperatures 2.09 K and 2.10 K. The critical value of $\dot{M}$ at which value bulk HeII leakage began seemed to become smaller as the temperature T_B rose. Such bulk leakage in a form of intermittent spouts resulted in an abrupt increase in $\dot{M}$. This behavior is also clearly recorded in Fig. 21-c, in which data points at these two temperatures tend to approach to the saturated vapor pressure curve while those at other temperatures do to deviate from the curve as the temperature at the downstream side, T_P, drops. These two particular behaviors, sudden increase in $\dot{M}$ and sudden change in p_P approaching to the saturation vapor pressure, are regarded as general signs of the leak state, in addition to visual observation of the existence of bulk HeII at the downstream side of porous-plug.

This particular porous-plug differs only in a number of basic parameters and the material from other porous-plugs as seen in Table 1. It does not seem that the difference in the plug material plays a decisive role. There were, in fact, no noticeable distinctions in the flow characteristics between the two kinds of porous-plugs at lower temperatures. The crucial parameters must be the thickness and possibly the permeability of the porous-plug. The thickness must be too small to prevent bulk HeII from leaking through it. The permeability may be slightly too large. The balance between the pressure gradient, which is the driving force to make the forward flow, and the temperature gradient must be lost because of the small thickness and the large permeability. A

porous-plug whose thickness is too small and the permeability is too large may fail to prevent bulk HeII from leaking through it especially at higher temperatures. The condition in which HeII leakage occurs depends, of course, on T_B, p_B, T_B-T_P, p_B-p_P and $\dot{M}$ as well as the thickness and the permeability.

3.7 Vapor-Liquid Phase Boudary inside of Porous-Plugs

It has been the basic assumption that the location of the vapor-liquid phase boundary just coincided with the downstream side of the plug. Thus, the two quantities, $(p_B-p_P)/l$ and $(T_B-T_P)/l$, have been regarded as the pressure gradient and the temperature gradient developed as a result of liquid HeII flow through a plug. However, several experimental evidences suggest that the phase location should be inside of plugs. The pressure at the downstream side p_P, was, in fact, below the saturation vapor pressure corresponding to the temperature there, T_P, except for cases with small $\dot{M}$. Thus, the pressure gradient of (liquid) HeII was much overestimated. The experimental result that all the measured data are below the theory as shown in Fig. 20 may partly be attributed to this. In addition, the total temperature drop, T_B-T_P, is so large that it may be unrealistic to consider it develops only in the liquid phase. The experimental values are larger than those predicted by London's relation, Eq. (18), by two orders of magnitude. The fact that the mass flow rate is proportional to square root of the total pressure drop may be interpreted as to be associated with a turbulent flow through porous material for large mass flow rate. It was also observed that bulk HeII which was spouted through a plug was completely sucked into porous-plug by the following appearance of spouts. Thus, it may be a natural conclusion that the phase boundary is located inside of a plug. Furthermore, the location varies depending on the flow condition, and the vapor phase flow through a part of plug is sometimes dominant over the liquid phase flow with respect to the total pressure and themperature drops. On the other hand, the state of the phase surface should not be always steady nor be the configuration flat. The schematic illustration of the phase boundary is given in Fig. 22. A realistic configuration must be inbetween the two extreme cases indicated by (a) and (c) in this figure, that is (a) is the case that the plug is almost saturated with liquid HeII and some leakage may appear and (c) is of nearly dry out. The two extreme cases were also certainly realized in some

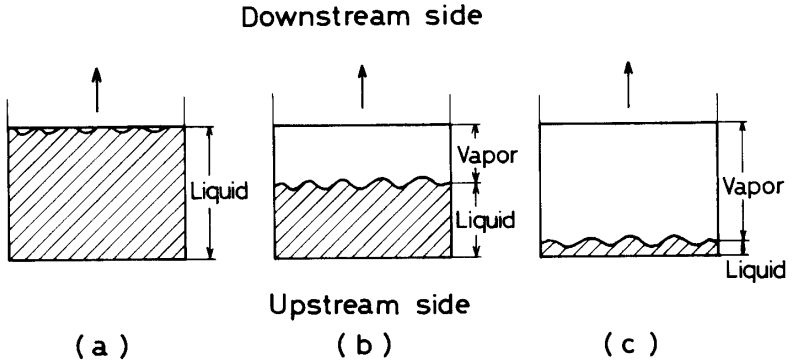

Fig. 22. Schematic illustration of the vapor-liquid phase boundary inside of a porous-plug. (a); nearly saturated, (b); realistic configuration, (c); nearly dryout.

cases. It naturaly follows that every quantity measured in this experiment should be regarded as a mean value averaged in the time and the space.

IV. Flow Rate Control by the Use of a Heater

There is a counter flow system of liquid HeII inside of a porous-plug. One is the forward flow of the normal component, and another is the backward flow of the super component which is driven by the thermomechanical effect caused by the temperature difference across a porous-plug. It is natural to consider that if the effect is controlled by any means, a control of the flow rate of the super component and thus of the total mass flow rate may be possible. In this experiment, a method of heating at the downstream side of a porous-plug by an electric heater was attempted. It is the fundamental idea that the flow rate of the super component must be decreased by rising the temperature at the downstream side and, therefore, the total flow rate be increased. The basically identical apparatus and experimental procedures as the basic research were employed to conduct this experiment. The measurement was carried out at several temperatures, T_B, while changing the heater power. The detail of the porous-plug section with a heater is illustrated in Fig. 1. The heater was winded on a copper reel, which was thermally isolated except that it was thermally contacted to a copper disk on the downstream side of the plug. It may be considered that all heat generted by the heater was not consumed for

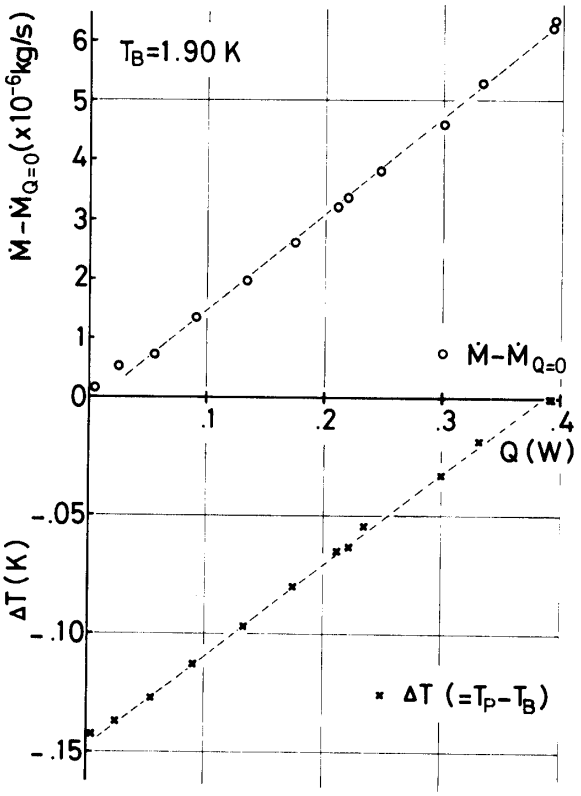

Fig. 23. Effect of heating on the flow rate and the temperature difference. This experiment was carried out by making use of a specially designed porous-plug. $A=8.31\times10^{-3}$m, $K=2.13\times10^{-13}$m^2.

controlling action but some portion may be extracted while the vapor flows through holes of the copper disk.

The first result given in Fig. 23 is an example to explain the quantitative efect of heating on the flow rate and the temperature at the downstream side. The heat input, Q, is taken as abscissa, only a prt of which may be utilized for the control. The ordinates are the temperature difference, ΔT ($=T_B-T_P$), and the net gain of the mass flow rate $\dot{M}-\dot{M}_{Q=0}$, respectively. Here, $\dot{M}_{Q=0}$ is the mass flow rate under the condition of $Q=0$. Any conditions of the vapor flow passage and the temperture, T_B, were unchanged during this experiment. The result shows that the mass flow rate increases and ΔT decreases with Q. At heating rate above a critical value, which was 0.39 W for this particular case, the liquid HeII was observed to leak through the plug, when ΔT became nearly zero. It was confirmed that the control of the flow rte through porous-plug was basically feasible by the use of a heater.

The data given in Fig. 24 is a regular ($\dot{M}-\nabla p$) plot of a result of the experiment which was carried under a fixed condition of the control valve opening while the heat input was changed from 0 W to a value at which liquid leakage occurred. In this figure, circles represent the data of the case with a medium vapor flow conductance, which started from the upper branch, and x's do those from the lower branch. Both data traces are almost identical within the experimental error. Another experimental result for the case with a higher conductance was also shown in this figure by crosses. HeII leakage began when the pressure drop across the plug disappeared. This experiment shows that a fairly wide

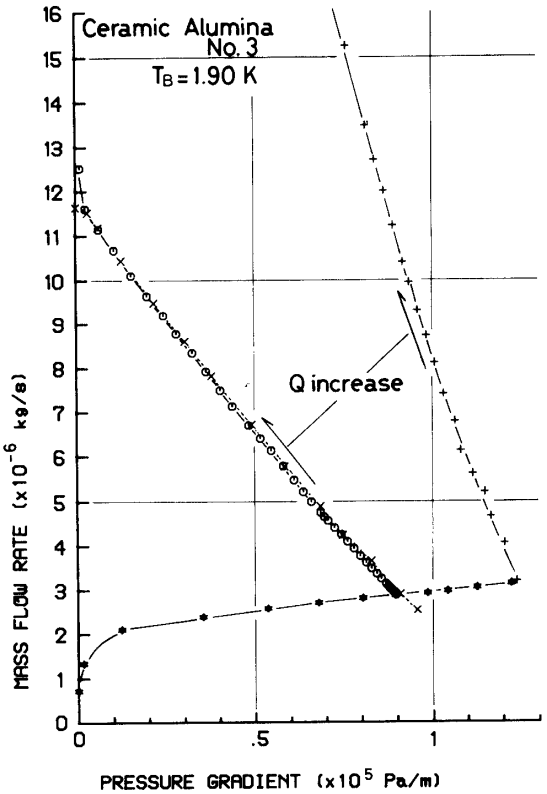

Fig. 24. Variation of the mass flow rate with heat input at two fixed vapor flow configurations.

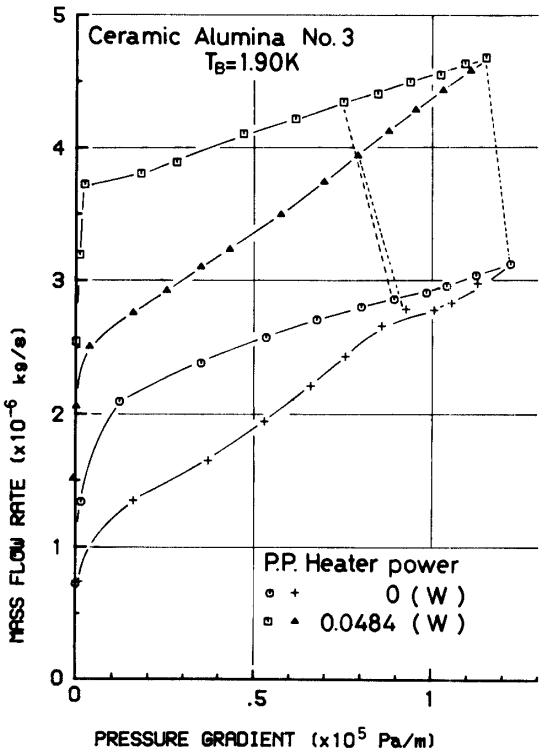

Fig. 25. Effects of heating on the steady flow characteristics.

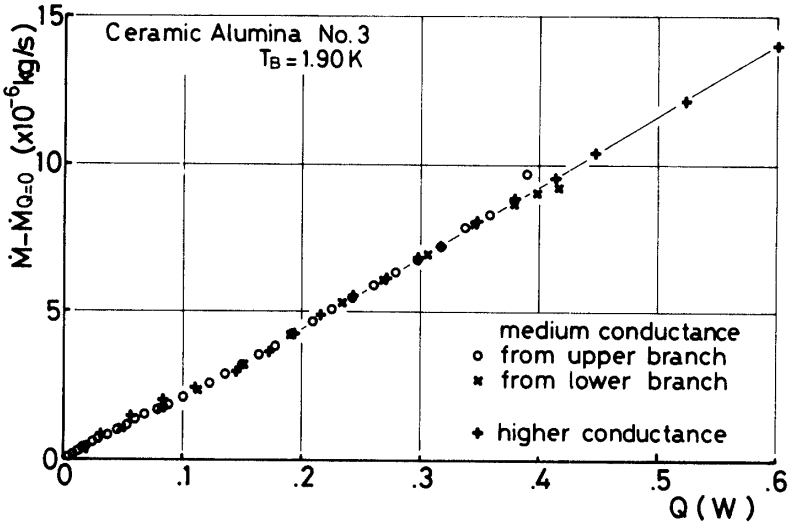

Fig. 26. Variation of the net augmentation of the mass flow rate, $\dot{M}-\dot{M}_{Q=0}$, due to heating with heat input Q. Two vapor flow conditions, one for medium flow conduction, and another for higher conductance.

range of the flow rate control can be attained by this method. Effects of heating on the steady flow characteristics are given in Fig. 25. The measurement was made under two heating conditions, Q=48.4 mW and 0W, at a constant bath temperature, T_B. Corresponding two data points under the same valve opening condition, one for Q=0 and another for Q=48.4 mW, are connected by dotted lines for each valve condition. It is quite evident from this figure that the general flow characteristics, that is the $\dot{M}-\nabla p$

relation, are qualitatively almost unaffected by Q and that the value $\dot{M}_0$ is, however, predominantly increased by heat addition. The hysteretic character still appeared under heating condition. The variation of the net augmentation of the mass flow rate, $\dot{M}-\dot{M}_{Q=0}$, with heat input, Q, is shown in Fig. 26 on two conditions of the vapor flow passage at a temperature, $T_B=1.90$ K. It is of great interest to find from this figure that all data points lie on a single curve independent of the initial condition whether it started from the upper or lower branch and of the vapor flow conductance. The maximum attainable augmentation of the flow rate, at which value liquid leakage begins, is larger for higher vapor passage conductance.

It is confirmed from these experiments that the mass flow rate control by the use of a heater is, in principle, feasible and that the mass flow rate can be augmented by a couple of times. In the case that precise and wide range control of the mass flow rate is required in space missions, a heater could be used to increase the flow rate as well as control valve on the vapor flow passage.

V. Porous-Plug Experiment in Zero-Gravity aboard a Rocket

Rocket flight experiments had been demanded to understand the zero-gravity behavior of superfluid helium and to define actual problems concerning to launching helium cryostat in the course of the basic study of IRTS (Infrared Telescope in Space) program [9]. An onoard experiment was attempted, in which the observation of dynamic behavior of liquid helium (HeII), the verification test of a porous-plug plase separator with a controlling heater, the investigation of the heat transfer and the breakdown of superfluid thin film, and the noise test of a cooled FET pre-amplifier for IR detectors were performed. The detailed report has already been published (Ref. 1). The experimental cryostat was launched by a sounding rocket S-520 in February of 1982. The motor burnout occurred at 32 sec after launch and the payload section was separated from the booster at 60 sec. Every component of the acceleration was basically less than $10^{-3}\times g_0$, where g_0 is the gravity acceleration on the ground, during the free flight for about 400 sec. The porous-plug was a disk shaped ceramic alumina (22-mm-dia and 6-mm-thick), which was designed based on the ground test data. It was fixed in the porous-plug mount, and a heater for flow rate control and a thermometer, T_4, were installed at the downstream side. The schematic illustration of this section is given in Fig. 27. The flow rate through the plug was designed to be about 2.5×10^{-6} kg/s, which was equivalent to a cooling power of 50 mW at about 2.0 K. HeII in the main vessel was evacuated by a rotary pump to keep the temperature at about 2.0 K until the launch. The evacuation line for the porous-plug venting was shut-off just before the launch, and then it was mechanically opened into space after 60 sec. The temperature history is shown in Fig. 28, where T_1 is the temperature of liquid HeII and T_6 that on the outer wall of the HeII vessel. It was not until 120 sec that effective evacuation through the porous-plug from the vessel resumed as seen form the figure. Liquid HeII having leaked into a dead space in the downstream side during the period when the venting line had been closed was firstly evacuated, which dried out by 120 sec. It is fair to say that the porous-plug actually worked as a phase separator because T_1 dropped monotomously and

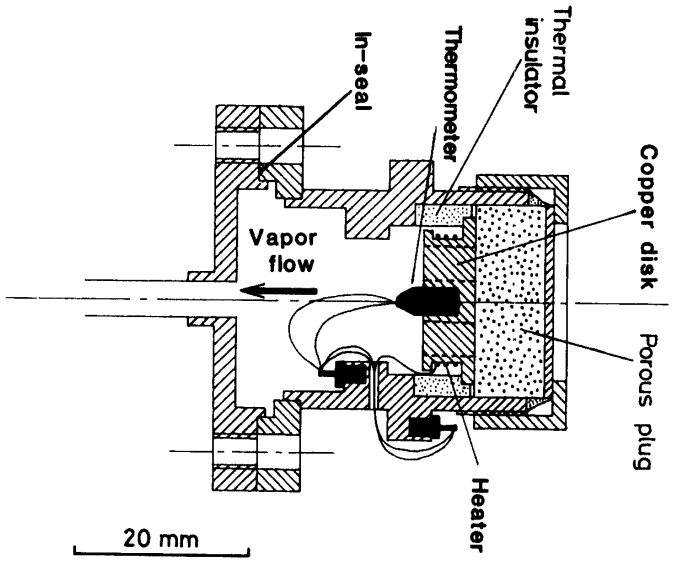

Fig. 27. Structure of onboard porous-plug phase separator.

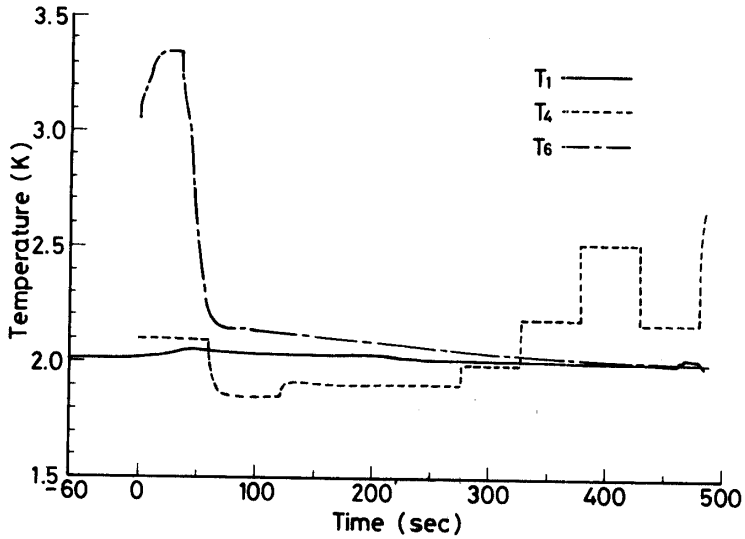

Fig. 28. Temperature history in HeII vessel. T_1; HeII temperature, T_4; porous-plug temperature at the downstream side, T_6; outside wall temperature of the HeII vessel.

T_4 was always lower than T_1 except heating period after 280 sec. Programmed heat input to the downstream side of the plug was stepwise applied from 280 sec to investigate the effects on the flow. The heat input levels are 5 mW, 16 mW and 33 mW, respectively. However, the flow rate data could not be obtained because of malfunction of the flow meter. It can be, neverthless, confirmed from the data of T_4 that the porous-plug performed the function as well as phase separation even for the highest heating rate. This heating rate had always resulted in overheating to lead to dryout in the laboratory tests when the porous-plug had been placed above the HeII surface. It is confirmed from this zero-gravity experiment that the porous-plug really acts as a phase separator in the zero-gravity state and that it is possible to control the flow rate by a heater. This flight experiment also verified that the porous-plug was compatible with the

inertia force and vibration imposed during the powered flight, and that the results from basic experiments on the ground were of use for the design of onboard porous-plugs.

VI. Conclusions

The conclusions which could be made based on the experimental results may be summarized as follows.

i) The HeII phase separation was satisfactorily performed by the use of porous-plugs so far as they were activated through the vapor evacuation.

ii) Two branches of the flow characteristics are recognized according to whether the mass flow rate is being increased or decreased, which bring about a flow hysteresis.

iii) The flow characteristics (the $\dot{M}-\nabla p$ relation) are categorized into four regions; 1) the creeping region ($\nabla p=0$), 2) the onset of the normal component flow (the transition to the non-linear region), 3) the non-linear region, 4) the linear region.

iv) The hysteresis feature cannot be recognized in the $\nabla T-\nabla p$ relation. The overall temperature drop is considerably larger than that predicted by the London relation.

v) There is a flow region in which $\dot{M}\neq 0$ while $\nabla p=\nabla T=0$ (the creeping region).

vi) In the linear region, the gradient, $(\dot{M}-\dot{M}_0)/\nabla p$, is always smaller than the theoretical values. This seems to suggest the recession of the vapor-liquid phase boundary into the inside of plugs.

vii) In the non-linear region, the 1/2-power law holds in the $\dot{M}-\dot{M}_0$ vs ∇p relation.

$$\dot{M}-\dot{M}_0=C_\alpha A(K)^{1/4}(\rho_{sat})^{1/2}(\nabla p)^{1/2}$$

viii) The vapor-liquid phase boundary is located somewhere inside of plugs and is unsteady, and the configuration of the boundary may be rather complex than flat.

ix) It is feasible to cnsiderably increase the mass flow rate due to heat addition to the downstream side of the porous-plug.

x) The mass flow rate in the creeping region is predominantly increased by heat addition and consequently the whole $\dot{M}$ curves shifted by this amount. The quantitative feature of the flow characteristics does not essentially change.

xi) The mass flow rate is augmented as the heat input is increased, but bulk HeII finally starts to leak out through for large Q when $\nabla p=0$.

xii) Porous-plugs could perform the perfect phase separation in the zero-gravity state and were compatible with severe inertia force and vibration during the rocket powered flight.

xiii) The data of the ground experiments are of use for the design of onboard porous-plugs.

Acknowledgement

This research was conducted as a part of the IRTS (Infrared Telescope in Space) program during the course of the basic research. The authors wish to express their appreciation to the Institute of Space and Astronautical Science for the encouragement and financial support.

REFERENCES

[1] M. Murakami, N. Nakaniwa, S. Hayakawa, T. Matsumoto, H. Murakami, K. Noguchi, K. Uyama and H. Nagano, "Zero Gravity Experiment of Superfluid Helium", ISAS Rept. No. 604, The Inst. of Space and Astro. Science, June 1983.

[2] H. D. Denner, G. Klipping, I. Klipping, K. Lüders, J. Menzel, U. Ruppert and H. Walter, "Performance of an Active Phase Separator for Helium", Proc. of ICEC8, 1980, pp. 32–37.

[3] H. Denner, G. Klipping, K. Lüders, D. Petrac, U. Ruppert, U. Schmidtchen, Z. Szücs and H. Wlater, "Investigation of HeII Phase Separation Instabilities", Proc. ICEC9, 1982, pp. 186.

[4] D. Petrac and P. Mason, "Evaluation of Porous Plug Liquid Separators for Space Superfluid Helium Systems", Proc. of ICEC7, 1978, pp. 120.

[5] D. Petrac And P. Mason, "Temperature Control of Superfluid Helium on Zero-g by a Porous Plug", Proc. ICEC8, 1980, pp. 97.

[6] G. K. Karr and E. W. Urban, "Superfluid Plug as a Control Device for Helium Coolant", Cryogenics, 1980, pp. 266.

[7] J. B. Hendricks and G. R. Karr, "Characterization of Superfluid Porous Plug Performance", Proc. of ICEC9 1982, pp. 190.

[8] M. Murakami, N. Nakaniwa and K. Uyama, "Porous-Plug Phase Separator for Superfluid HeII", Proc. of ICEC9, 1982, pp. 194.

[9] S. Hayakawa, Proc. Symp. on advanced Instrumentation for Space Astronomy, Pergamon Press, 1982.

[10] U. Schotte and H. D. Denner, "The Mechanism Governing Phase Separation of Helium II by means of Narrow Channel", Proc. ICEC8, 1980, pp. 27.

[11] U. Schotte, "Common Flow Characteristics of Various Type of HeII Phase Separators", Proc. ICEC9, 1982, pp. 287.

[12] U. Schotte, "Mass Flow and Critical Velocity of Helium II in a Liquid Vapor Separating System", Z. Phys. B, Condensed Matter, 48, 1982, pp. 183.

[13] N. Nakaniwa, "An Experimental Investigation of Porous-Plug Phase Separators for HeII", the master thesis submitted to University of Tsukuba, 1983.

[14] R. B. Bird, W. E. Stewart and E. N. Lightfoot, "Transport Phenomena", John Wiley and Sons, New York, 1960.

[15] L. D. Landau and E. M. Lifshitz, Fluid Mechanics, Course of Theoretical Physics, Vol. 6, Pergamon, 1959.

[16] H. Schlichting, "Boundary Layer Theory", McGraw Hill, 1968.